



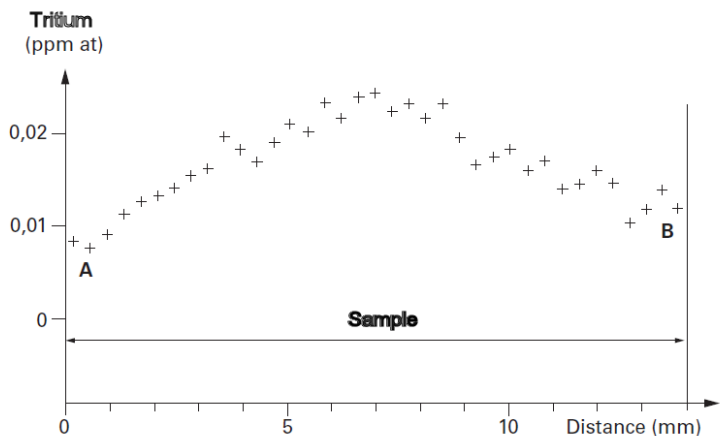
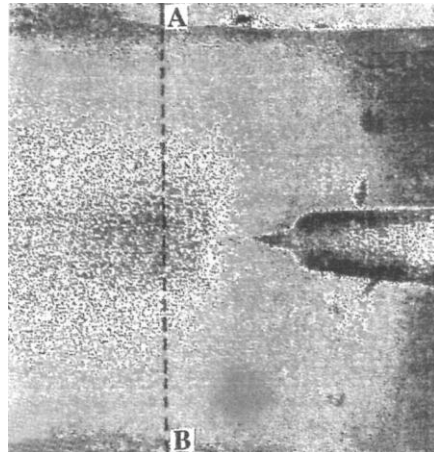
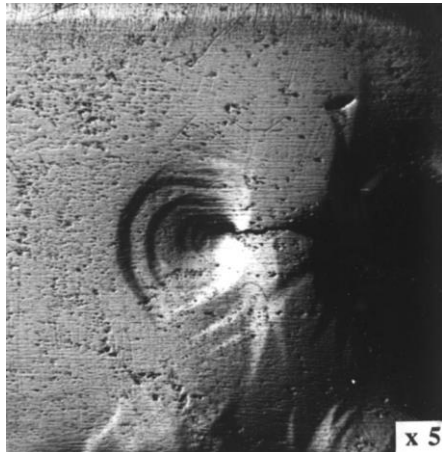
Hydrogen effects on the plasticity of model fcc and bcc alloys

David Delafosse

**Ecole des Mines de Saint-Etienne
Centre SMS, UMR CNRS 5307 : Laboratoire Georges Friedel,
158 Cours Fauriel, 42023 Saint-Etienne, France**



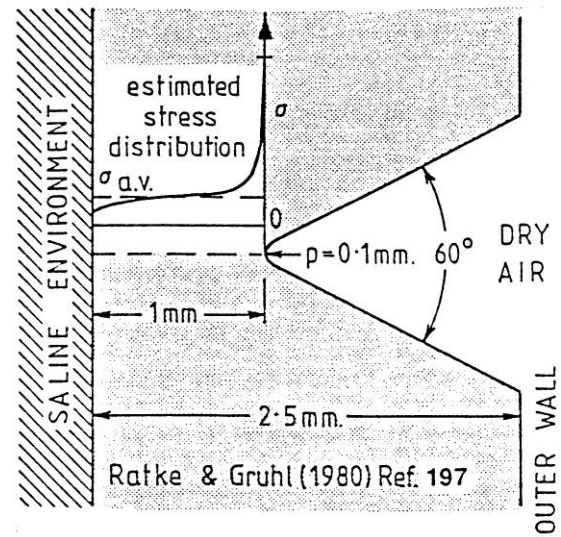
Historic Experiments



Tritium autoradiography in a crack-tip plastic zone

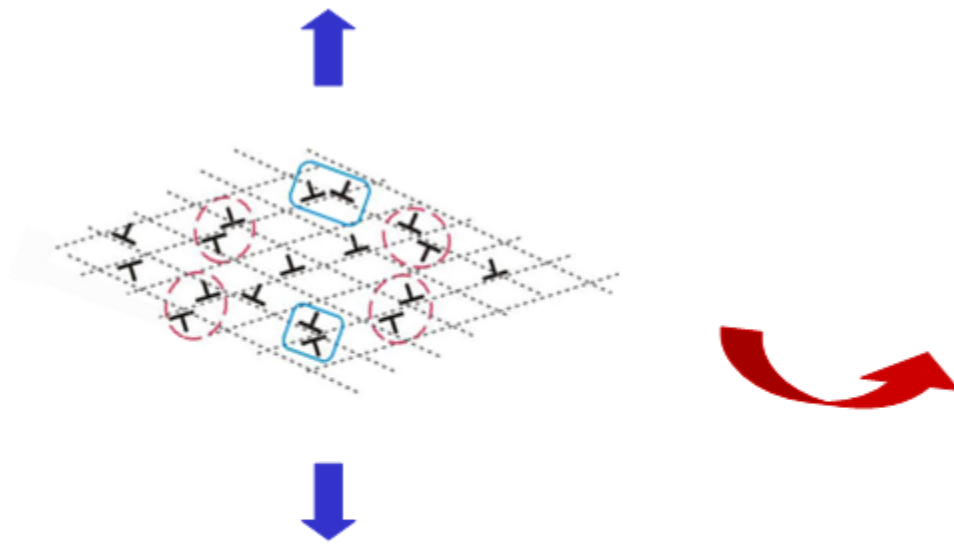
Chêne et al., J. Microsc. Spectrosc. Electron., 4 (1979) p. 37-50

H-diffusion in the hydrostatic stress-gradient ahead of a notch

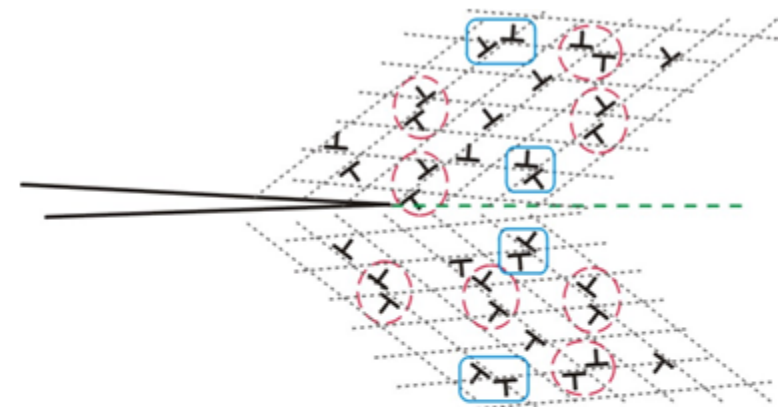


Gruhl, Z. Metallkd. 75, 11 (1984) p. 819

Implementation route for modelling H-effects on crack-tip plasticity



Step 1 : Implementation & validation
in uniaxial tension



Step 2 : Application to a cracked
bicrystal geometry

Experimental and analytical modelling of Hydrogen Effects on Tensile Properties

- 1. Elastic binding between mobile solutes and dislocations**
- 2. Modelling in the framework of the elastic theory of discrete defects**
- 3. H-effects on the tensile properties of fcc single crystals**
- 4. Slip localisation in fcc stainless steels**
- 5. H-effects on the plasticity of bcc FeCr**

Experimental & Modelling toolbox

Mechanical testing samples

> Model materials : Ni, Ni-16Cr, Fe-15Cr

High purity (less than 25 wt. ppm of impurity)

Single and recrystallised polycrystalline specimens

> Hydrogen charging in autoclave (450°C , P_{H2} = 150 to 200 bars, 48 hours)

Control of the hydrogen level and homogeneous concentration

Electrodeposited coating for bcc steels

> Testing at low temperature in a temperature chamber

Control of the temperature over large testing periods

Modelling background

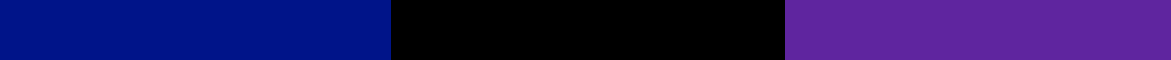
> Hydrogen effects : coupled elasticity-diffusion equations

(Larché & Cahn 85, Sofronis & Birnbaum 95, Chateau 2002)

Based on the elastic theory of crystal defects
Screening of dislocation pair interactions by hydrogen

> Plasticity mechanisms : line tension model (De Wit & Koehler 59, Friedel 64)

Simplified (but accurate) analytical description of the elementary plasticity mechanisms in FCC materials

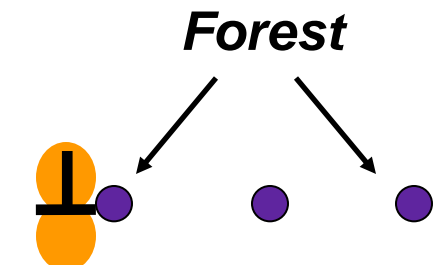


1. Elastic binding between mobile H solutes and mobile dislocations

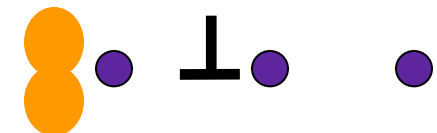
1. Dislocation pinning by H solutes

Dislocation ageing in fcc crystals

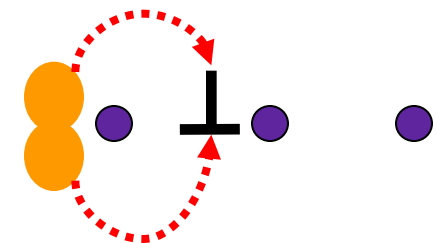
1 – Mobile dislocation pinned by **solute atmosphere**



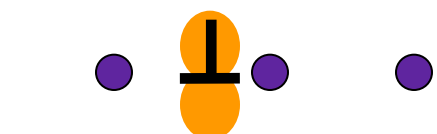
2 – Instantaneous jump of mobile dislocation between **Forest obstacles**



3 – Ageing of mobile dislocation by **diffusing** solute atoms during the time required for the thermally activated jump through **Forest obstacles**



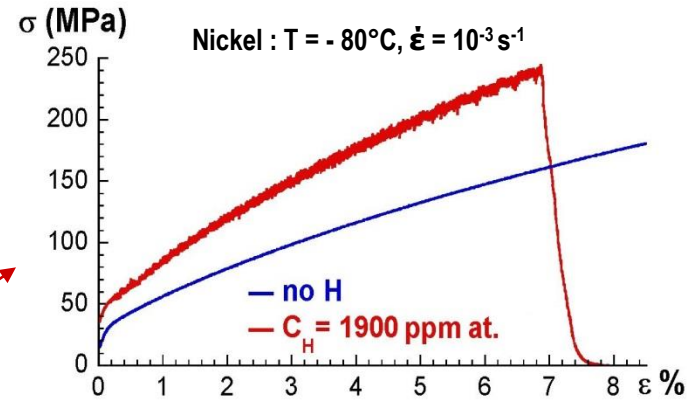
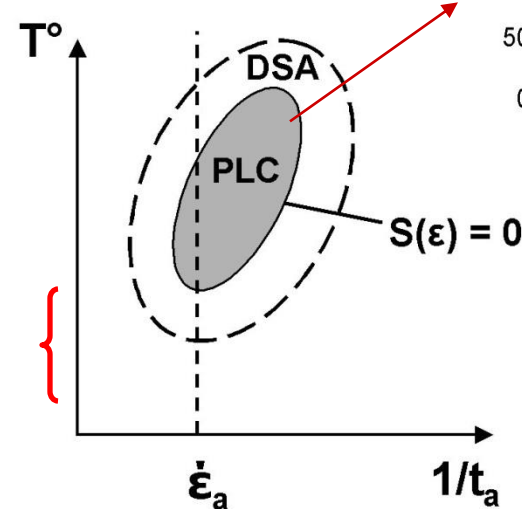
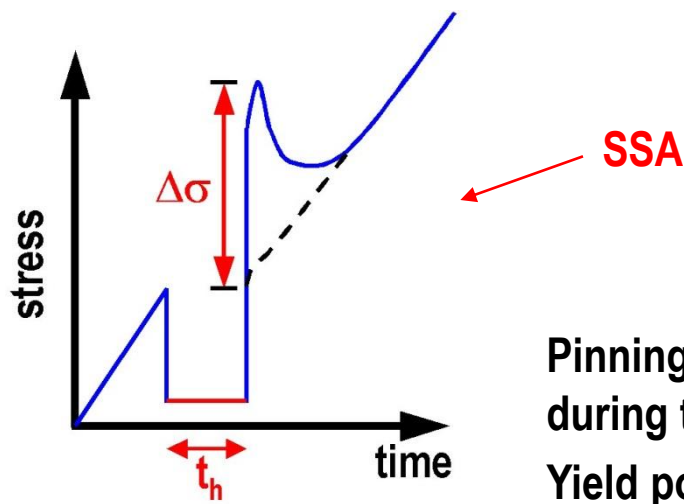
4 – Mobile dislocation pinned by **solute atmosphere**



1. Dislocation pinning by H solutes

Static Strain Ageing : SSA

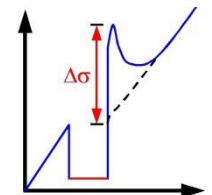
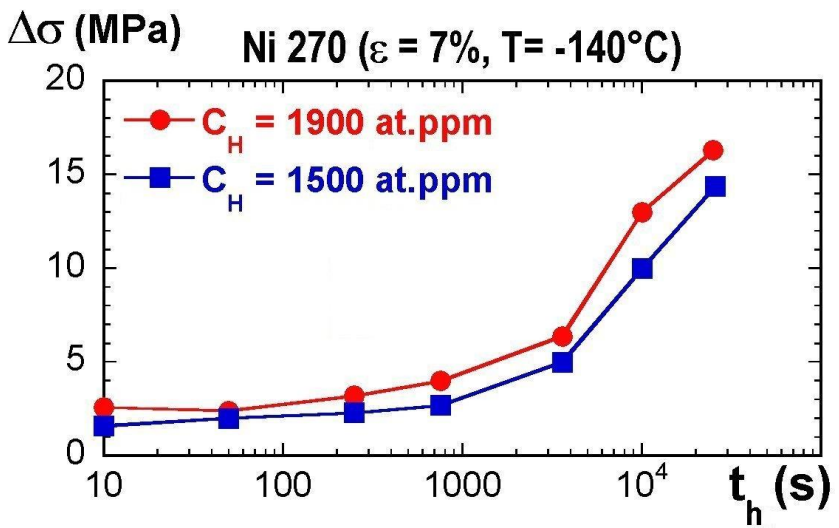
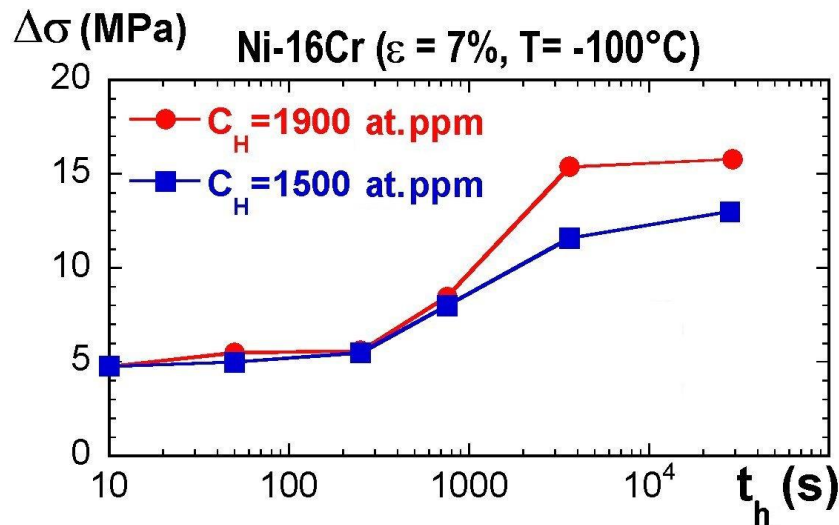
($T, \dot{\epsilon}$) domain where diffusing solutes no longer cope with mobile dislocations during continuous straining)



Pinning of dislocations by diffusing solute atoms during the holding time, t_h

Yield point, $\Delta\sigma$ = measurement of the pinning force

1. Dislocation pinning by H solutes



Ni-16Cr :

Saturation for $t_h > 10^4\text{s}$ at -100°C and 10^{-2} s^{-1}

→ $C_H = 1500 \text{ at. ppm} \rightarrow \sim 13 \text{ MPa}$

→ $C_H = 1900 \text{ at. ppm} \rightarrow \sim 16 \text{ MPa}$

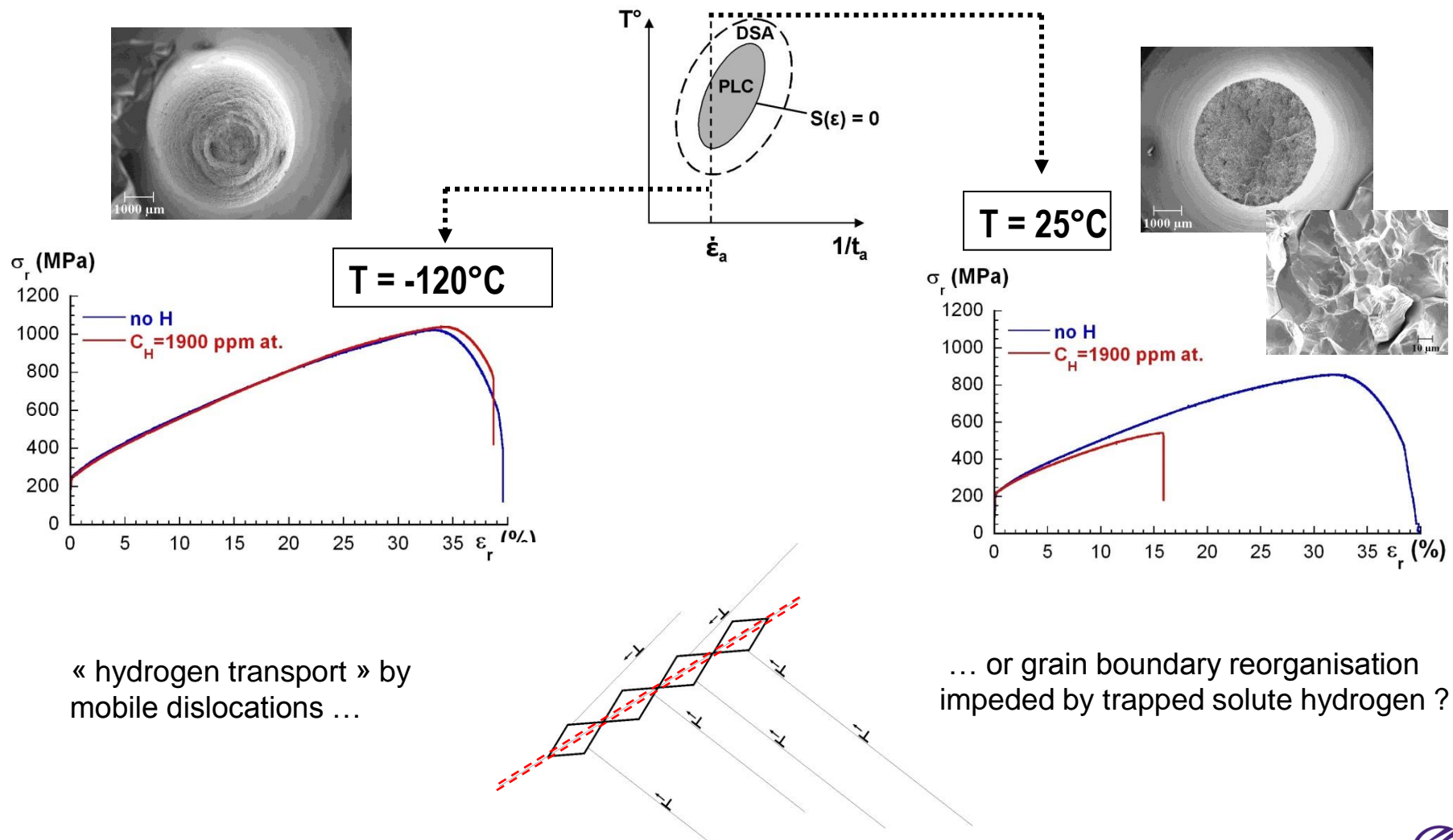
Ni :

No saturation at -140°C and 10^{-2} s^{-1} :

→ Saturation expected for $t_h > 10^5\text{s}$

→ Effect slightly higher for Ni than for the alloy

1. Consequences on Intergranular fracture



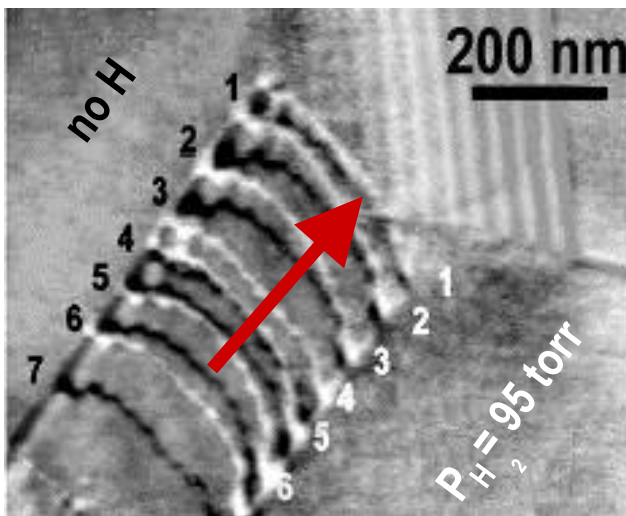


2. Modelling Hydrogen effects on elementary plasticity mechanisms in fcc metals

2. Problem statement

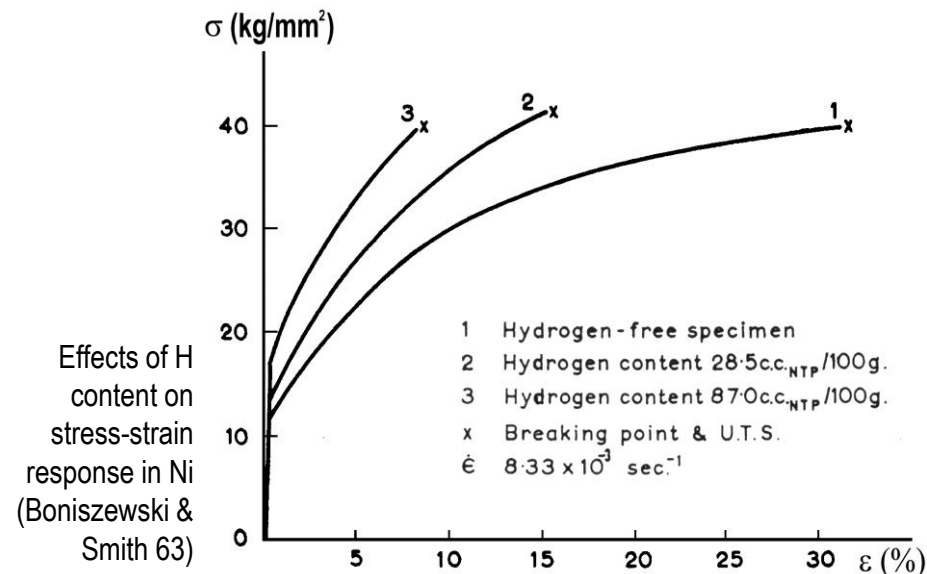
*Hydrogen Enhanced Localised Plasticity
mechanism for H-assisted fracture*

*based on the shielding of dislocation pair
interactions*



Influence
of H on
pile-up
density in
AISI 310s
austenitic
stainless
steel
(Ferreira
et al. 98)

*Macroscopic tensile response of
H-charged fcc alloys:*



> often referred to as a "**softening**" effect

> Macroscopic **hardening** is observed in (almost) all cases

2. Modelling H-dislocation interactions

Solute H ($r_H = 0.53 \text{ \AA}$) diffuses in octahedral sites ($r_s = 0.19 \text{ \AA}$)

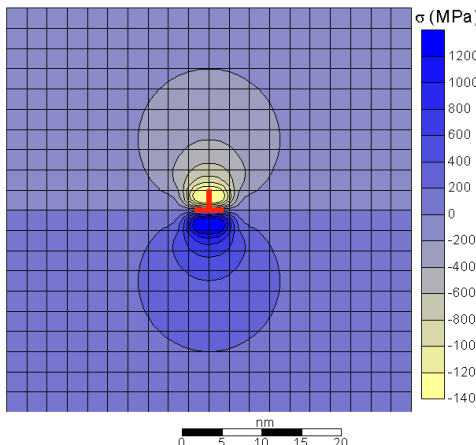
→ **Isotropic distortion of the host lattice : 1st order (elastic) effect**

Local H flux governed by :

- Concentration gradient
- Hydrostatic stress gradient

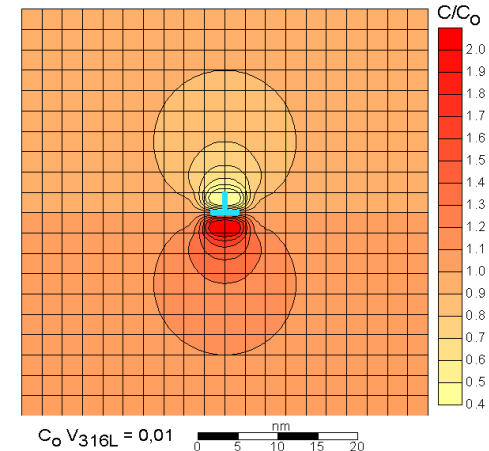
H diffuses in tension zones :

Hydrostatic stress field profile



- Segregation in the hydrostatic stress field of edge dislocations
- Relaxation of the hydrostatic stress

Steady state distribution

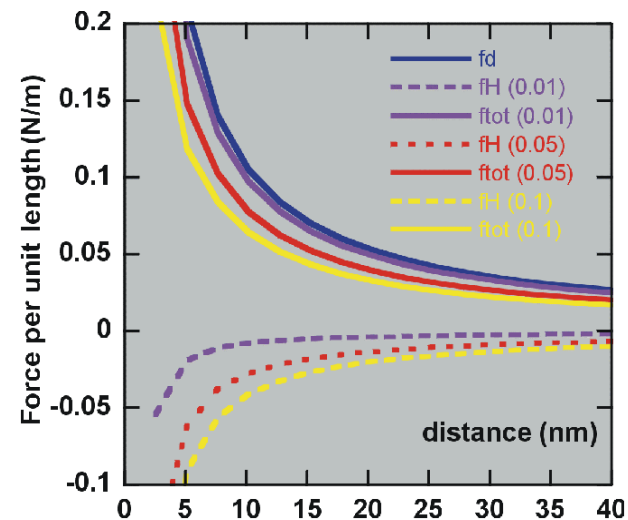


2. Modelling H-dislocation interactions

Screening of pair interactions

Associated stress profile of the same order than that of dislocations ($1/r$) with opposite sign : **screening of dislocations pair interactions**

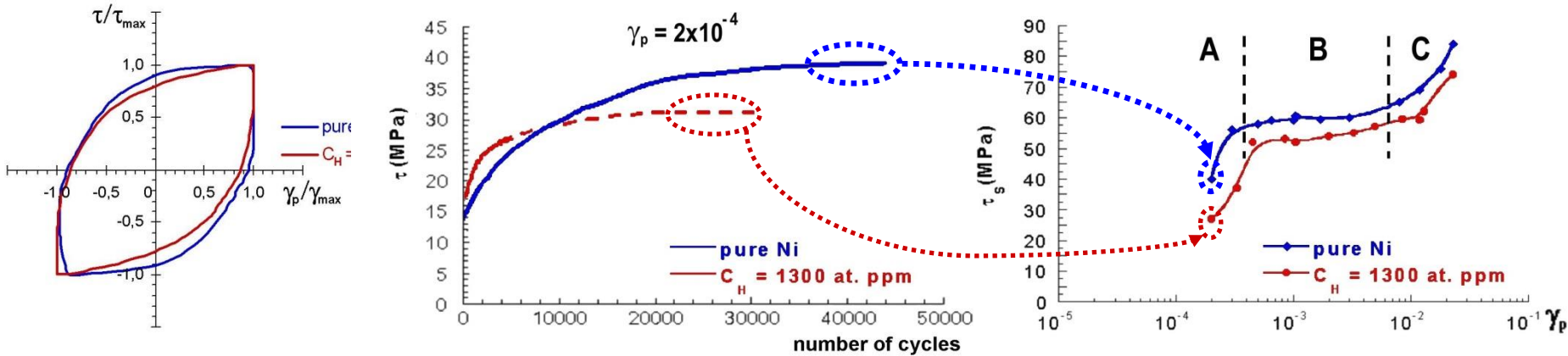
Relative screening effect = independent of the separation distance between dislocations



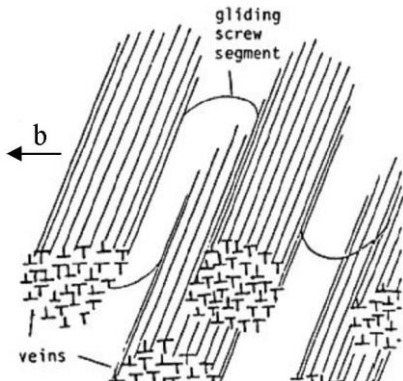
General expression for the screening of the resolved shear stress between the edge components of any dislocation pair

$$S(T, c) = \frac{S_0}{1 + \beta \frac{T}{c}} \quad \text{with } S_0 = 75\% \quad \beta = \frac{9(1-\nu)RV_M}{2EV^{*2}}$$

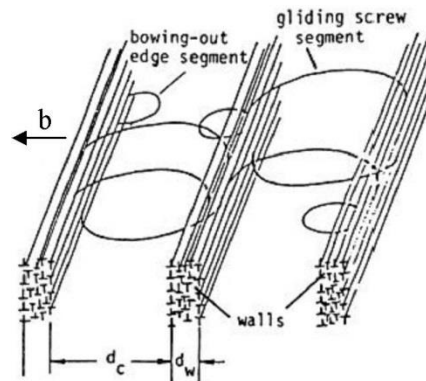
2. Cyclic plasticity in single crystals ...



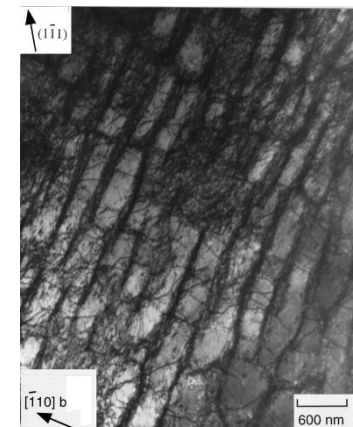
Region A :
Matrix-Vein structure



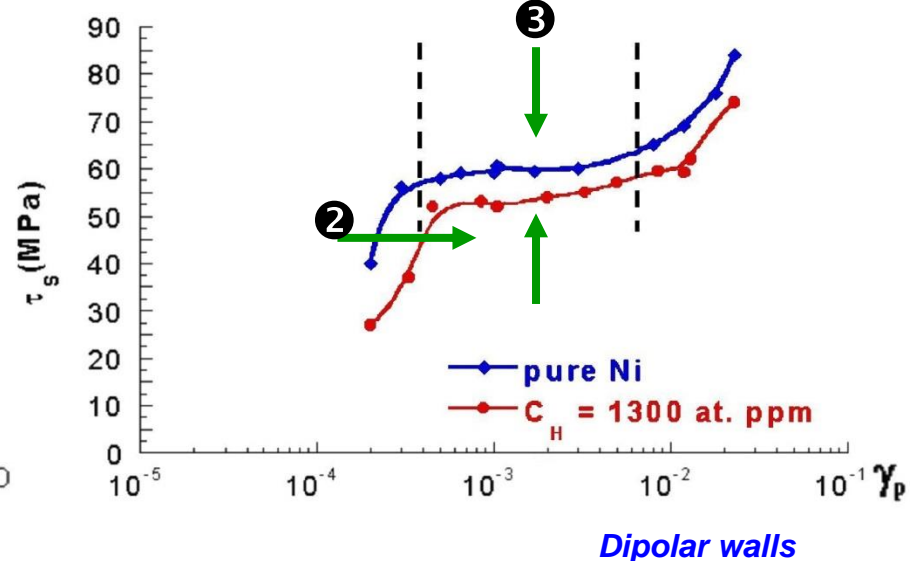
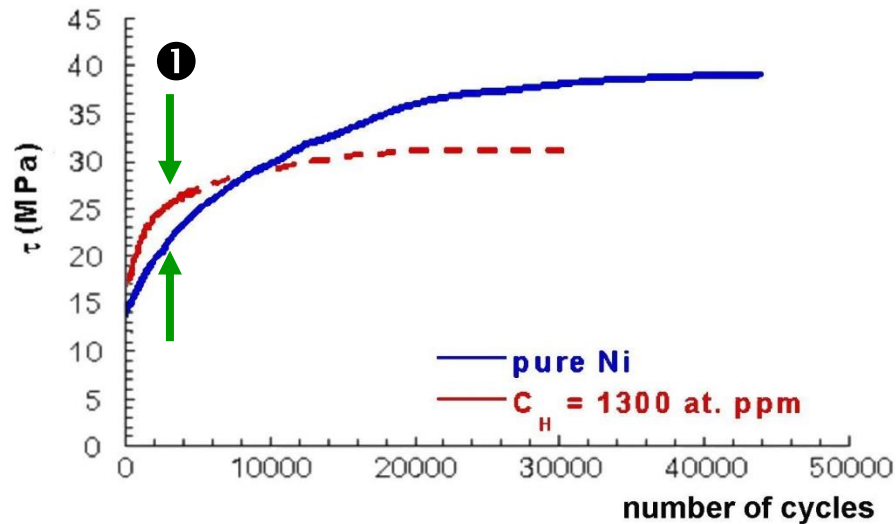
Region B :
PSB structure



Dipolar walls



... a (singular) direct consequence of the screening effect



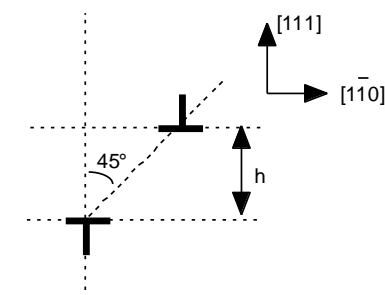
① ↗ of the initial cyclic stress amplitude (~10 MPa) : *Viscous drag of H atmospheres*

② Delayed dipoles formation and emergence of the PSB structure :

↘ cross-slip probability

↘ screening of elastic interactions

③ ↘ of τ_s (~10%) : increasing of dipoles size : ↘ screening of elastic interactions



$$h = \frac{\mu b}{8\pi(1-\nu)\tau}$$

2. Plasticity mechanisms

General expression for the screening of the resolved shear stress between the edge components of any dislocation pair

$$S(T,c) = \frac{S_0}{1 + \beta \frac{T}{c}} \quad \text{with } S_0 = 75\% \quad \beta = \frac{9(1-\nu)RV_M}{2EV^{*^2}}$$

→ Incorporating $S(T,c)$ in classical plasticity results

- > Line energy & Line tension (dislocation motion between forest obstacles)
- > Loop expansion (dislocation multiplication)
- > Stability of Junctions (hardening)
- > Separation and recombination of partial dislocations (cross-slip of screw dislocations)

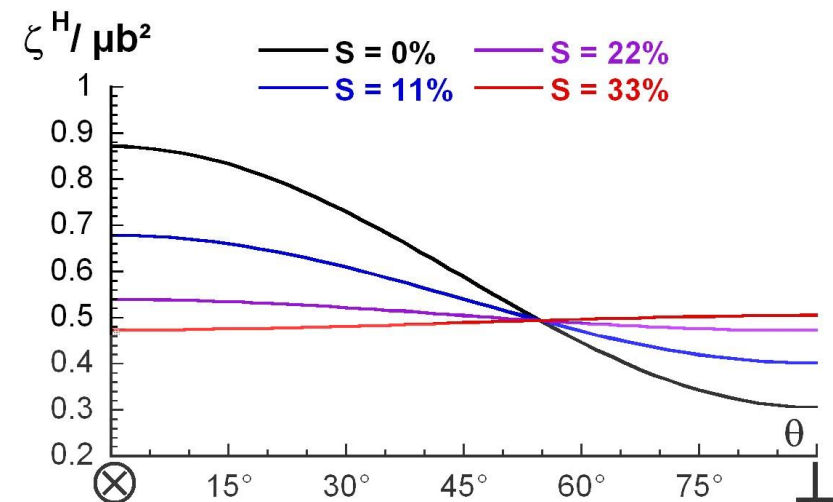
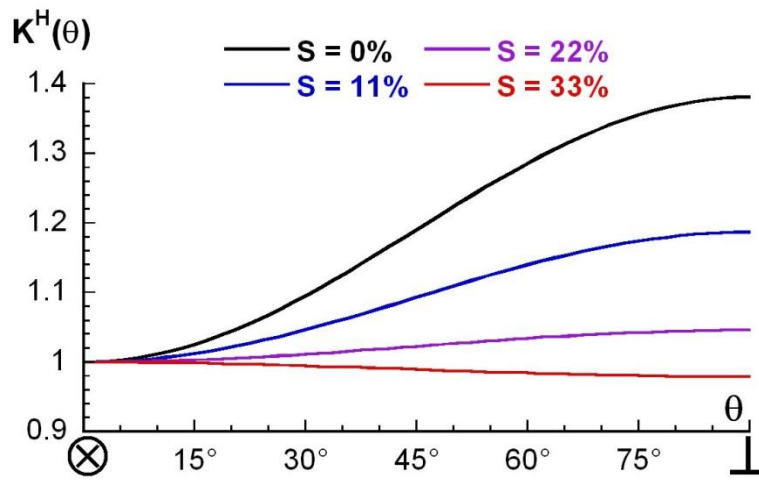
2. Line Energy & Line Tension

Self-energy $E(\theta)$ and line tension $\zeta(\theta)$:

$$E^H(\theta) = \frac{\mu b^2}{4\pi} K^H(\theta) \ln\left(\frac{R}{r_0}\right) \quad \text{with}$$

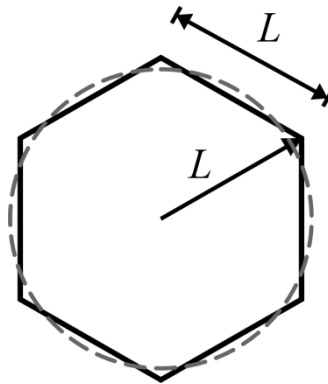
$$K^H(\theta) = \frac{1 - S(T, c) - (\nu - S(T, c)) \cos^2 \theta}{1 - \nu}$$

$$\zeta^H(\theta) = E^H + \frac{\partial^2 E^H}{\partial \theta^2} = \frac{\mu b^2}{4\pi(1-\nu)} \left[1 - 2\nu + S(T, c) + 3\cos^2 \theta (\nu - S(T, c)) \right] \ln\left(\frac{R}{r_0}\right)$$



2. Loop Expansion

Activation and expansion of Franck-Read dislocation loops



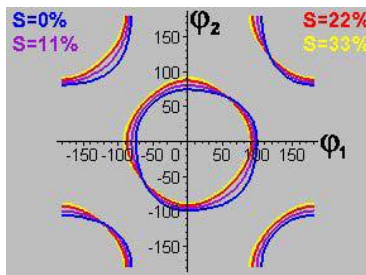
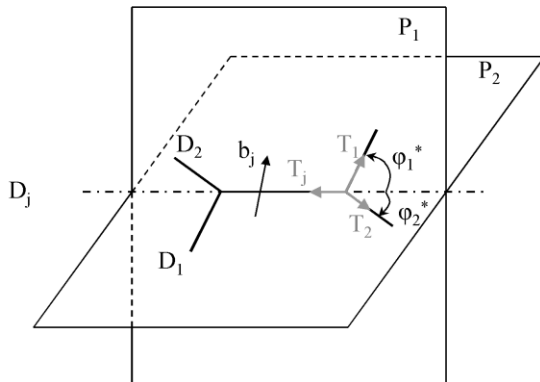
$$W^H = \frac{3\mu b^2 L}{4\pi(1-\nu)} \left[(2-\nu - S(T,c))(0.16 + \ln\left(\frac{L}{r}\right)\right]$$

**Decrease of the force for isotropic expansion
of dislocation loops in a line tension model**

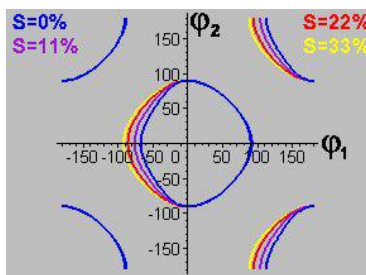
$$\frac{F^H}{F} = 1 - 0.58 S(T,c)$$

H in solution decreases the activation stress of Frank-Read sources

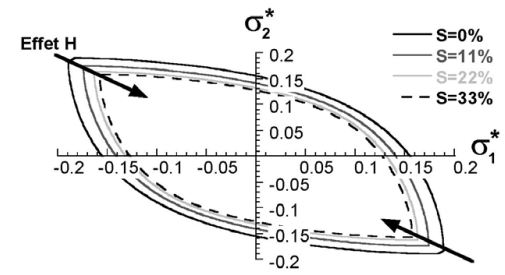
2. Formation and stability of dislocation junctions



Lomer

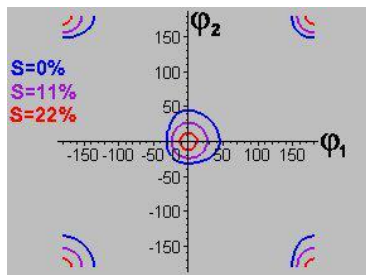


Glissile

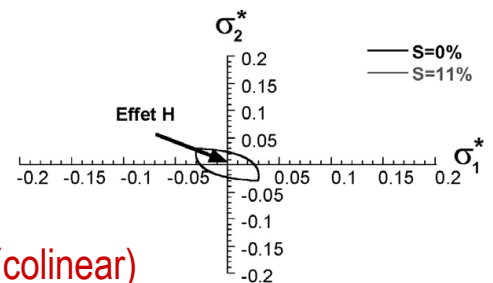


Condition for junction
« unzipping »

> Equilibrium of line
tensions at the triple
point



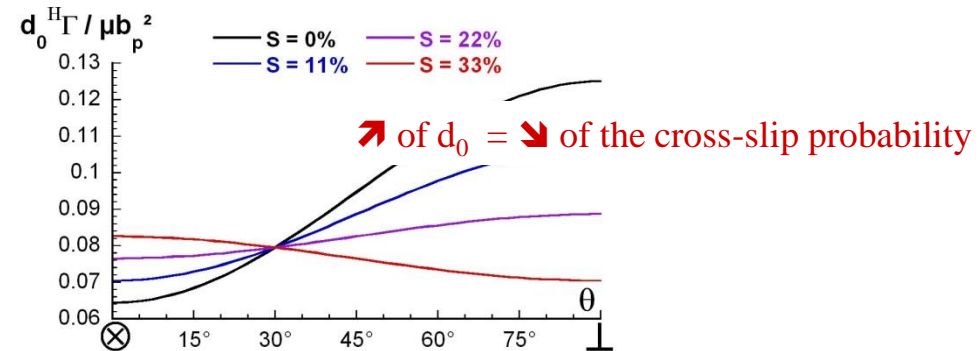
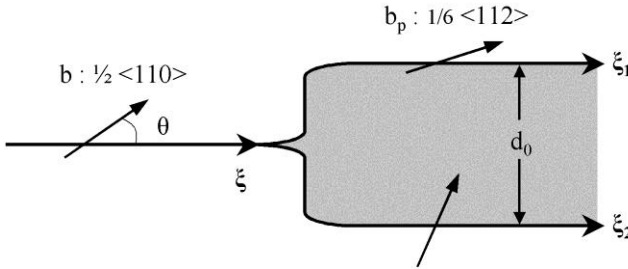
Hirth (colinear)



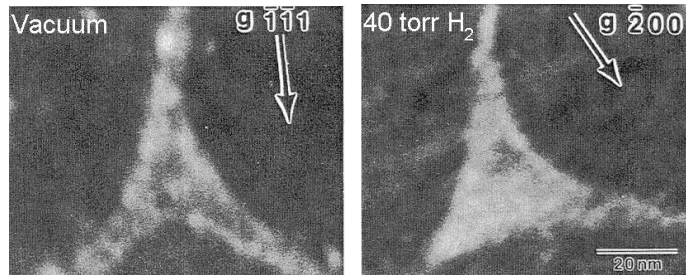
2. Cross-slip

Screening of interactions between partial dislocations

Assuming Stacking Fault Energy - Γ = independent of H concentration

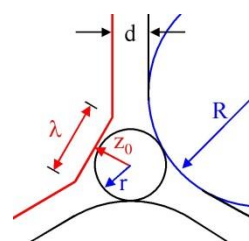


Influence of H on the equilibrium shape of an extended node



Ferreira et al. 96

$S(T,c) \sim 10\%$



Brown & Th\u00f6len model (SFE only) : \u2193 of Γ = 19%

With elastic effects : \u2193 of Γ = 26%

\u2193 of the cross-slip probability = core effects + elastic effects

Decrease of the cross-slip probability by combined elasticity and SFE effects

2. Summary

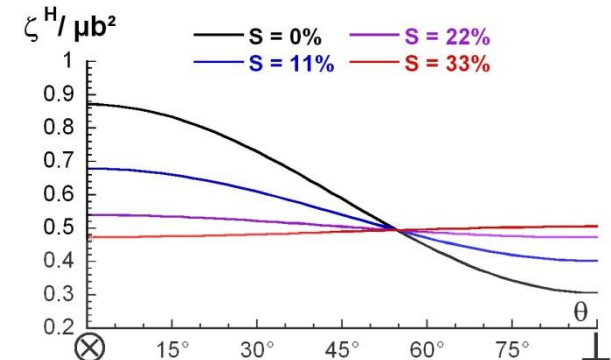
Screening index : $S(T,c) = \frac{S_0}{1 + \beta T/c}$

- Line energy $E(\theta)$ and line tension $\zeta(\theta)$:

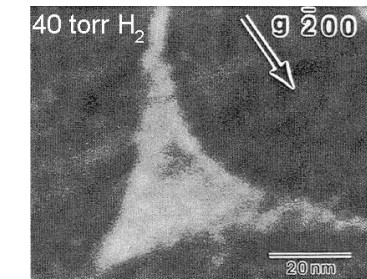
$$E^H(\theta) = \frac{\mu b^2}{4\pi} K^H(\theta) \ln(R/r_0)$$

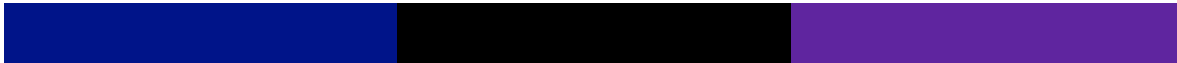
$$K^H(\theta) = \frac{1 - S(T,c) - (\nu - S(T,c)) \cos^2 \theta}{1 - \nu}$$

- H favours multiplication by Frank-Read sources :
- Moderate weakening of Lomer junctions for high values of $S(T,c)$, “collapse” of colinear junctions (first stage of hardening)
- Decrease of the cross-slip probability by combined effects on elastic interactions and SFE



$$\frac{F^H}{F} = 1 - 0.58 S(T,c)$$

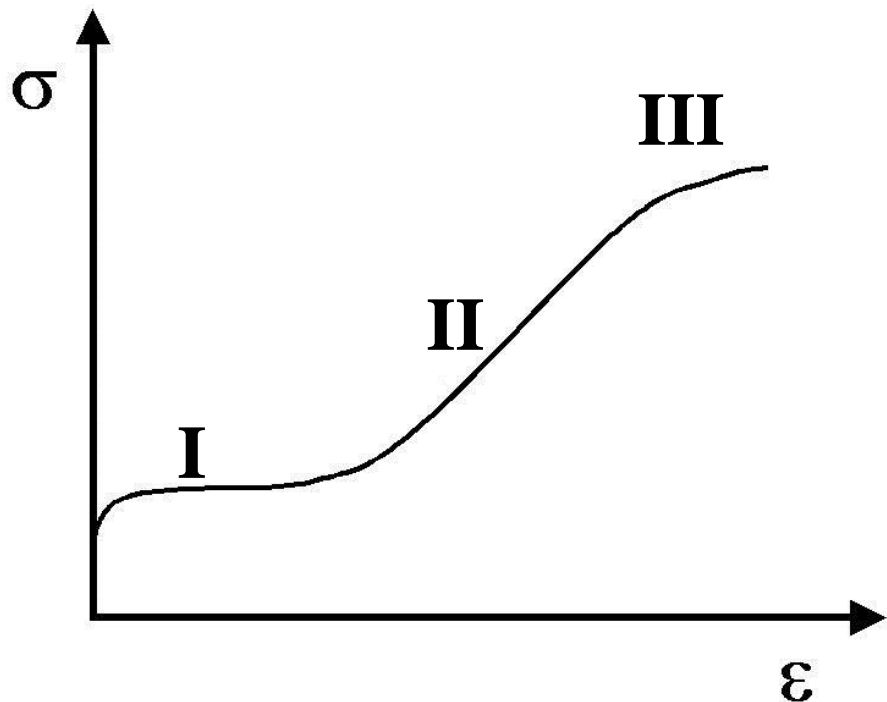




3. Tensile behaviour of H-charged f.c.c. single crystals

(coll. Xavier Faugeas, Université de La Rochelle)

3. Tensile behaviour of f.c.c. single crystals



Stage I : Planar Glide

- A unique slip system is activated
- Low hardening rate, controlled by multiplication and collinear junctions

Stage II : Linear hardening

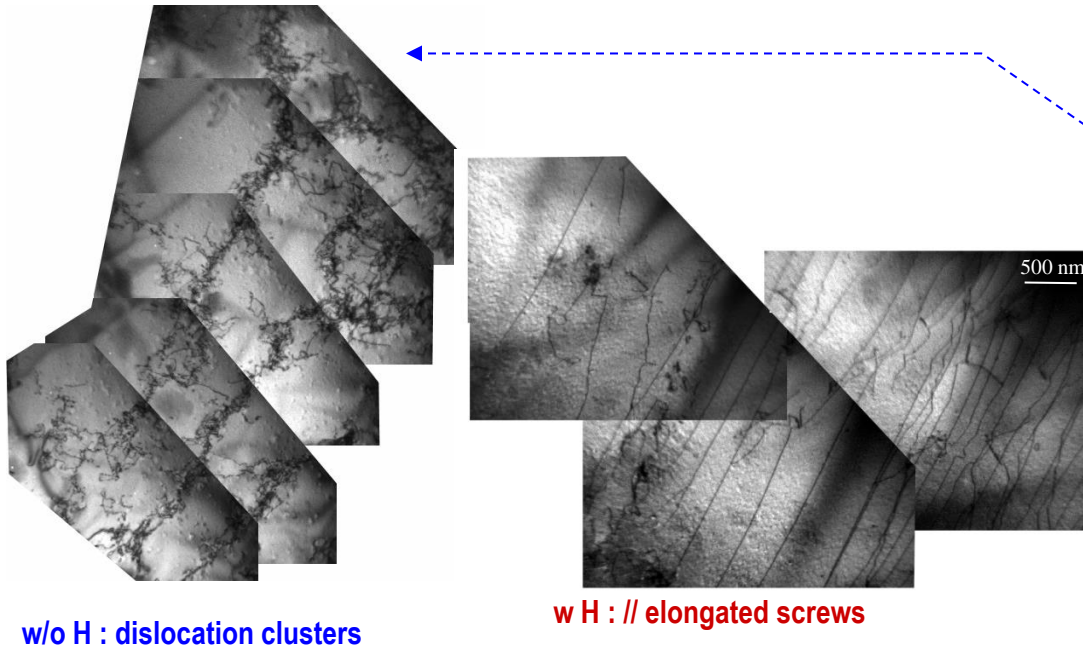
- Activation of secondary slip systems
- Hardening rate controlled by the spacing between Geometrically Necessary Boundaries (GNB)

Stage III : Parabolic hardening

- Strong influence of the cross-slip mechanism on the decrease of the work hardening rate

3. Tensile behaviour of f.c.c. single crystals – Stage I

Girardin & Delafosse 2004, Girardin Delafosse & Faugeas 2008

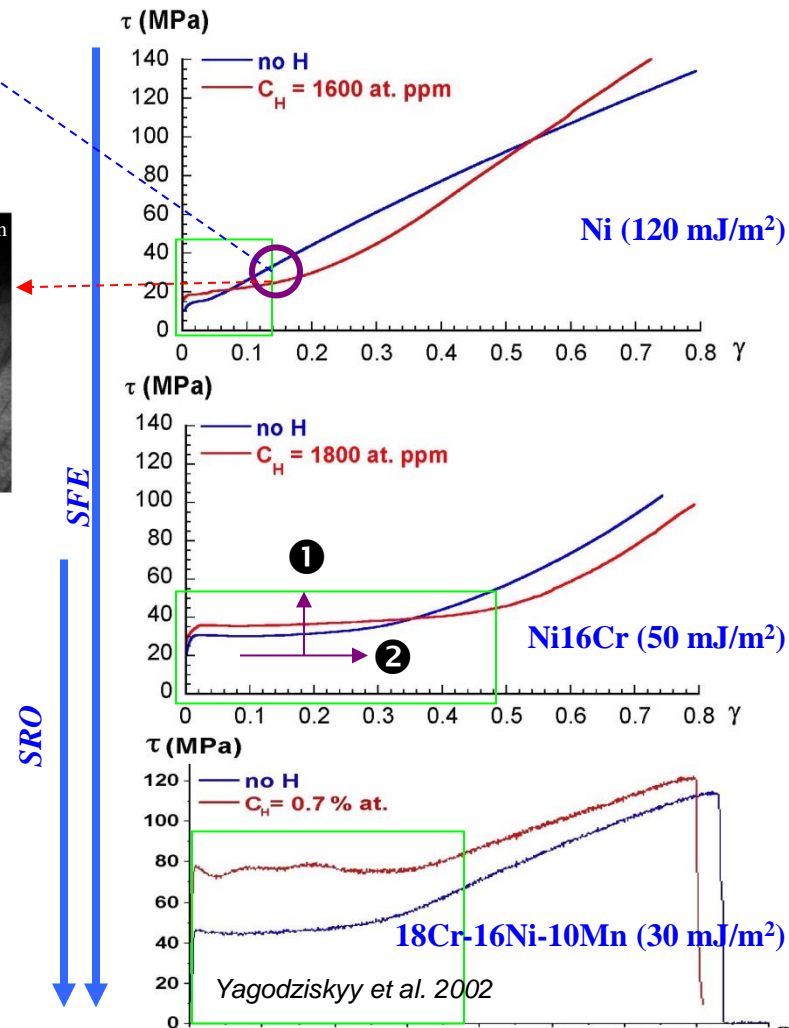


w/o H : dislocation clusters

w H : // elongated screws

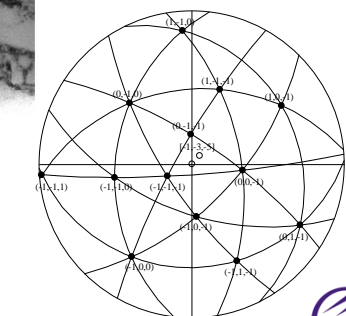
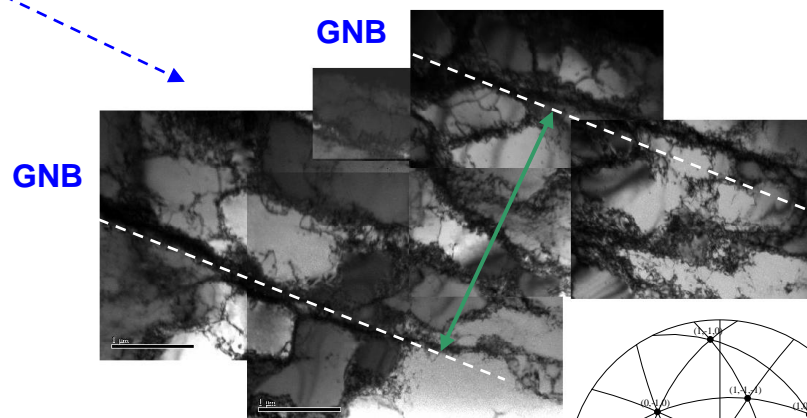
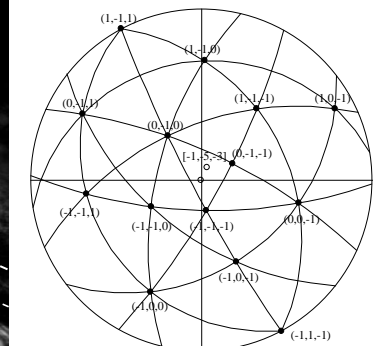
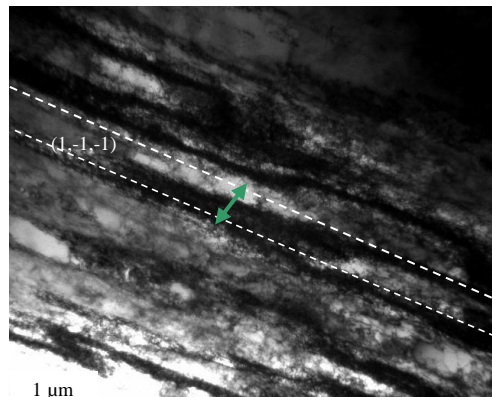
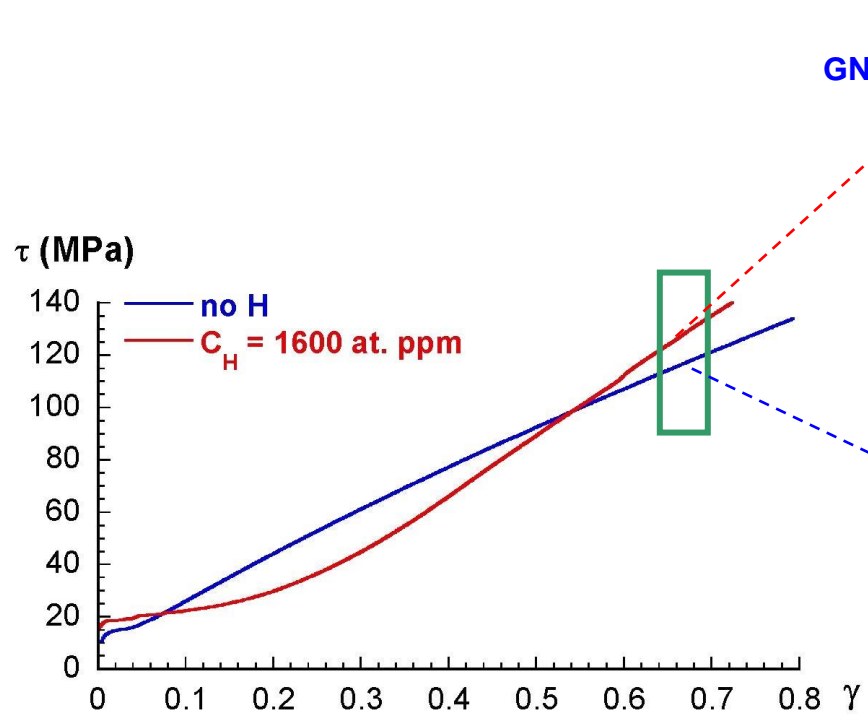
- ① ↗ of τ_I (~ 10 to 30 MPa, fct. of H concentration) :
Viscous drag of solute atmospheres

- ② Stage I extension:
Hydrogen favours planar glide and delays the transition to stage II



3. Tensile behaviour of f.c.c. single crystals – Stages II-III

Huvier, et al., Dislocation 2008, Hong-Kong

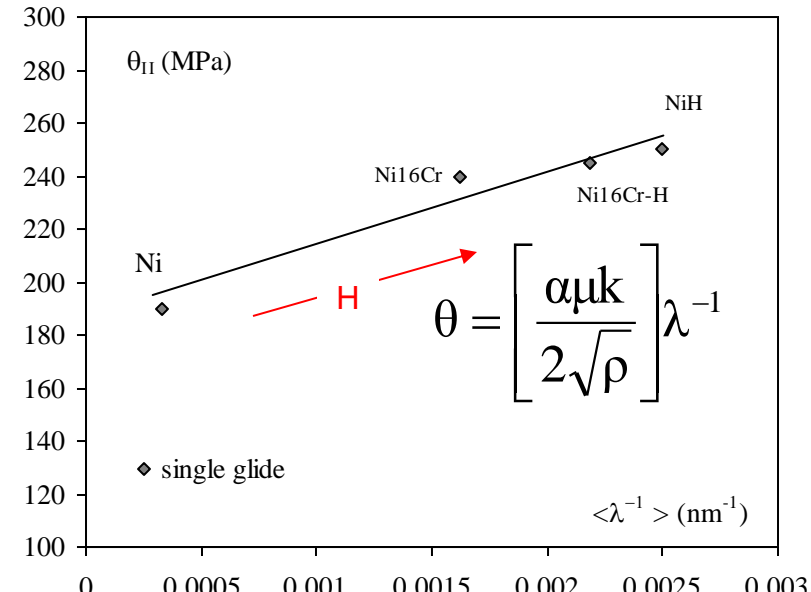
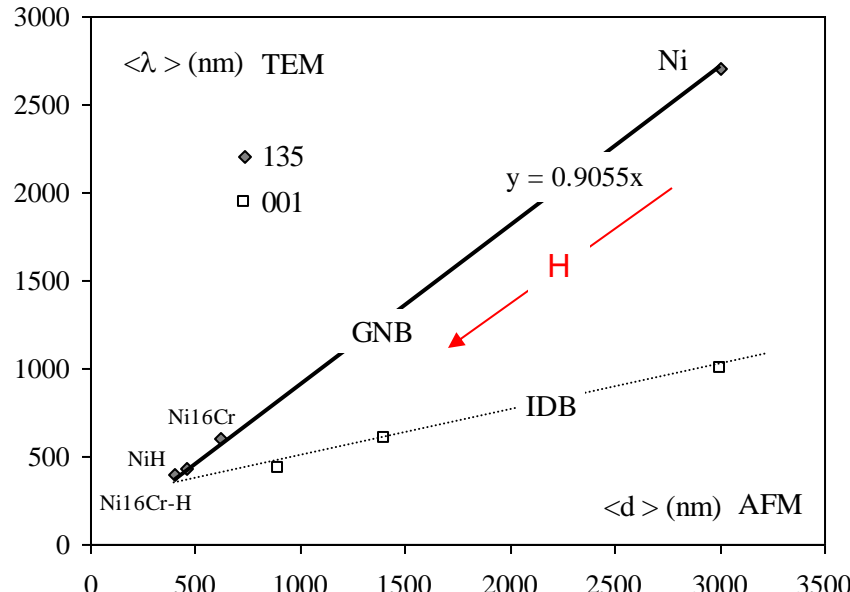


Hydrogen content decreases GNBS spacing (λ)

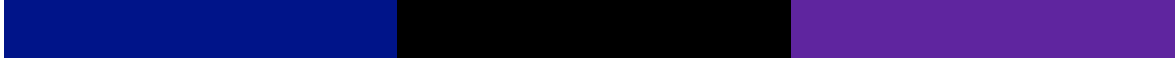
Equiaxed cells seem to disappear (controlled by the cross-slip)

3. Tensile behaviour of f.c.c. single crystals – Stages II-III

Huvier, et al., Dislocation 2008, Hong-Kong



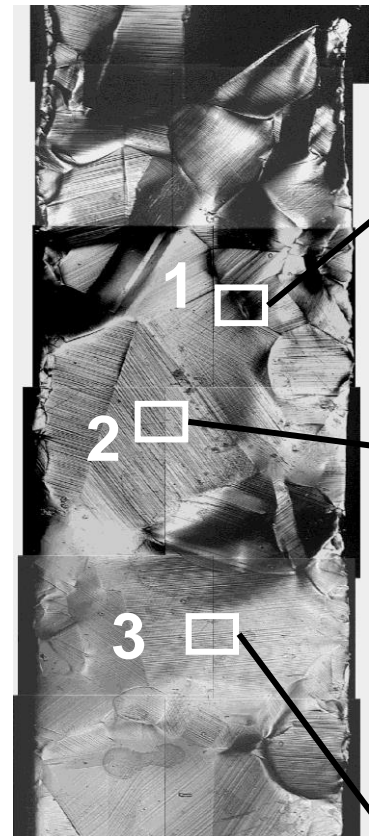
- Correlation between the inter- band spacing (d) and the inter-wall spacing (λ) :
GNBs act as a periodic distribution of barriers to dislocations motion.
- Hydrogen content decreases the inter- band spacing (d) and the inter-wall spacing (λ)
This effect decreases with a decreasing SFE (not observed for AISI 316L)
- The Hardening rate is a function of an internal length scale : λ



4. Slip Localisation in austenitic stainless steels

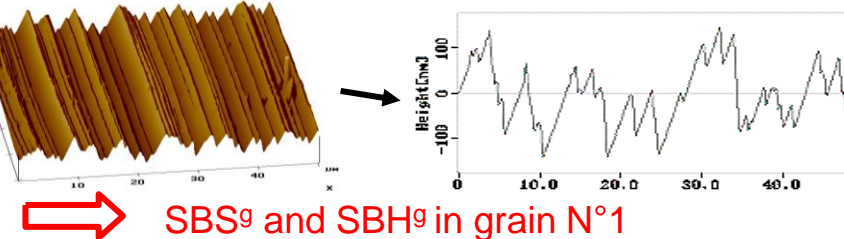
(JM. Olive, I. Aubert, N. Saintier, Université Bordeaux I)

4. Slip Localisation in 316L

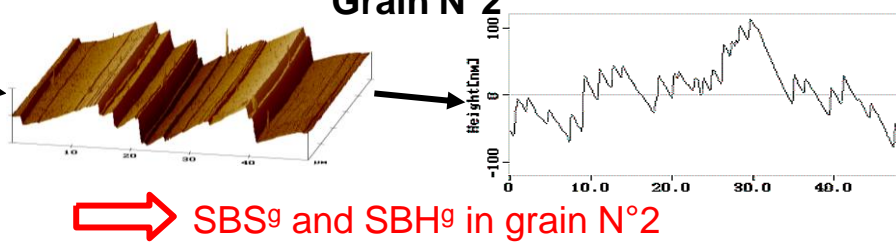


AFM observations

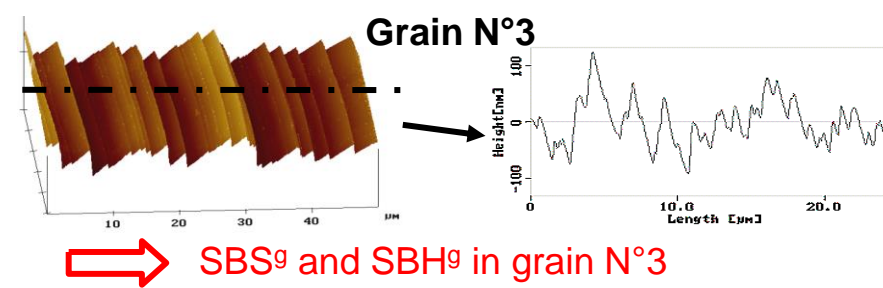
Grain N°1



Grain N°2



Grain N°3



Finite Elements
Calculation

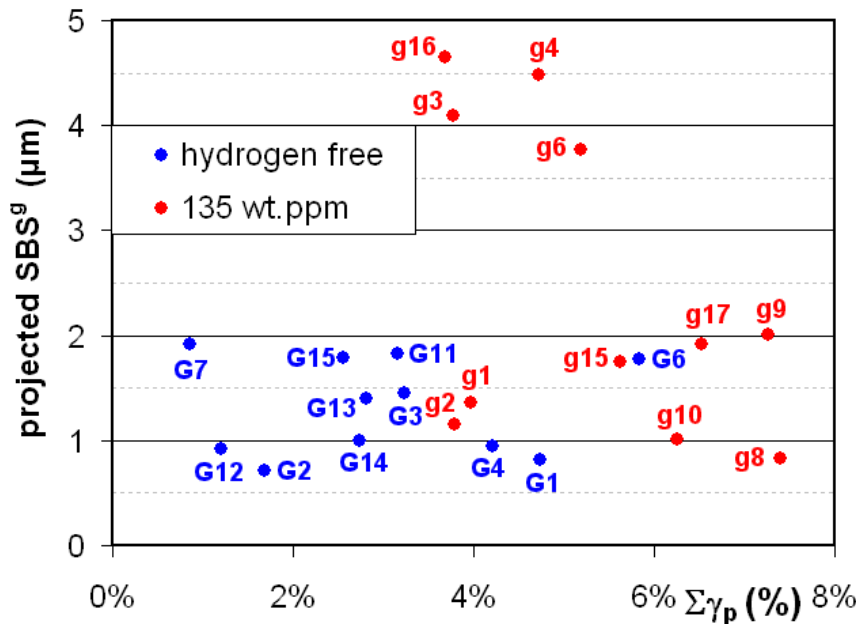
Plastic slip
in grain N°1

Plastic slip
in grain N°2

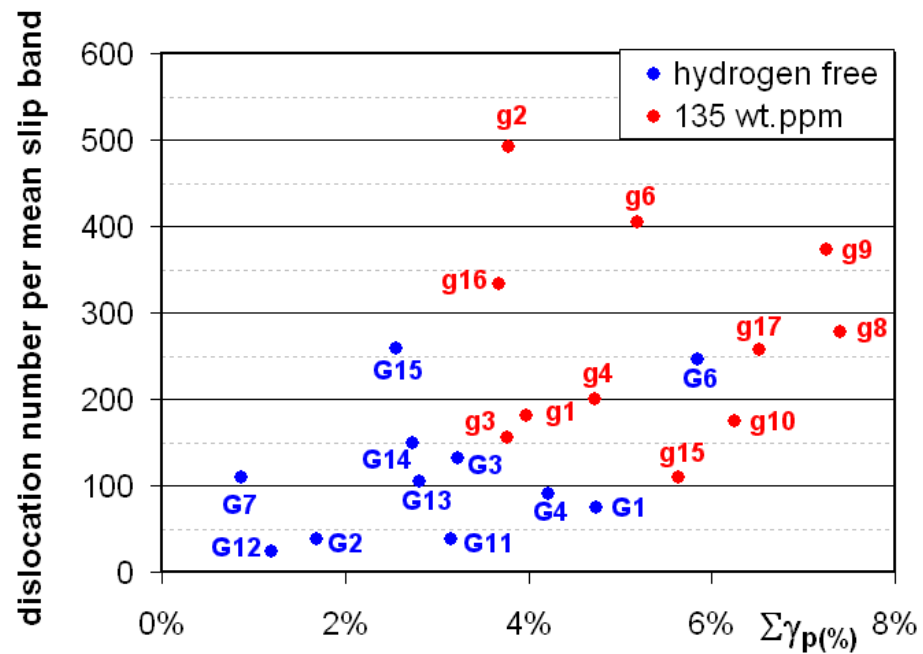
Plastic slip
in grain N°3

4. Slip Localisation in 316L

Projected SBS versus plastic shear



Number of dislocations per averaged surface step versus plastic shear



For the same total shear, Hydrogen-charged grains show twice as much projected Slip Band Spacing and twice as many dislocations per surface slip step as hydrogen-free grains

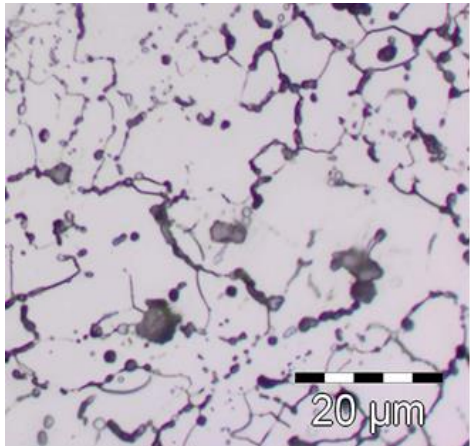


5. H-effects on the plasticity of bcc steels

- > *Sample preparation for H-charging*
- > *H-effects on dislocation multiplication*
- > *H-effects on the dislocation mobility*

5. Materials

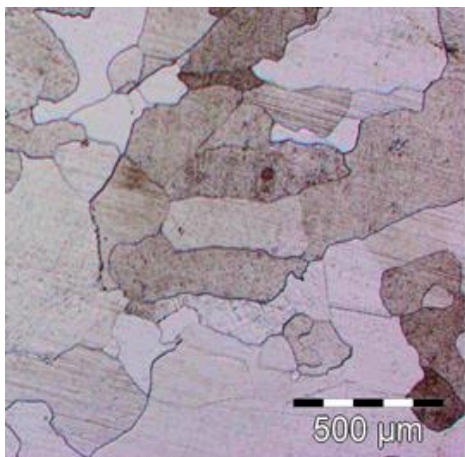
- **Ferritic stainless steel X14CrMo17 (AISI 430F)**



Large density of interfaces (matrix/precipitates)
maximizing hydrogen trapping

- **High purity ferritic binary alloy Fe15Cr**

Fe	Cr	C	O	N	S
matrix	14.97%	22ppm	12ppm	9ppm	2ppm



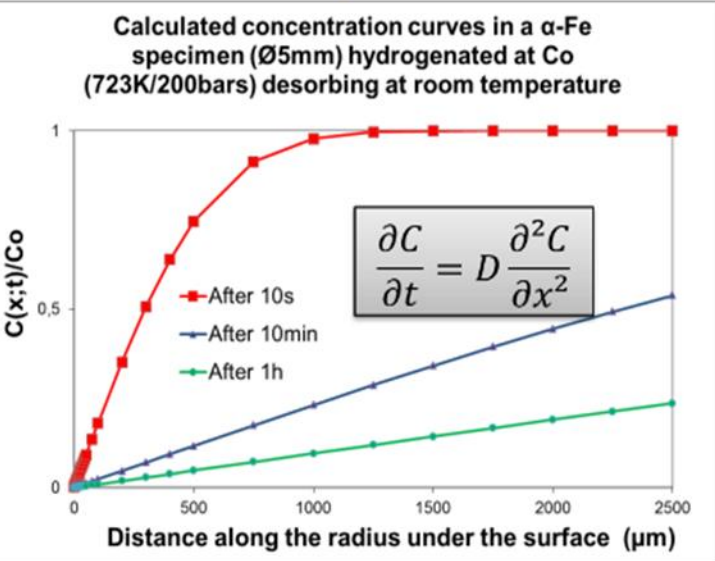
High purity material allowing an easier interpretation of the
hydrogen – dislocations effects

5. Sample preparation for H charging

Hydrogen diffusion rates and solubilities :

$$\begin{cases} D_{Fe_\alpha}(298K) = 9.6 \times 10^{-5} \text{ cm}^2/\text{s} \\ S_{Fe_\alpha}(723K/200\text{bars}) = 4.02 \text{ wt.ppm} \end{cases}$$

$$\begin{cases} D_{Ni}(298K) = 5.3 \times 10^{-10} \text{ cm}^2/\text{s} \\ S_{Ni}(723K/200\text{bars}) = 62.50 \text{ wt.ppm} \end{cases}$$

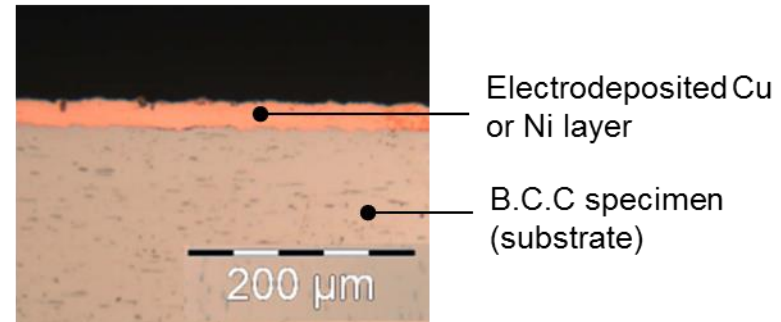


Hydrogen diffusion rates and solubilities in pure metals at atmospheric pressure:

$$D_{\alpha\text{Fe}}(298K) = 9.6 \times 10^{-5} \text{ cm}^2/\text{s} ; S_{\alpha\text{Fe}}(625K) = 1.3 \times 10^{-1} \text{ wt.ppm}$$

$$D_{Ni}(298K) = 5.3 \times 10^{-10} \text{ cm}^2/\text{s} ; S_{Ni}(625K) = 3.3 \text{ wt.ppm}$$

$$D_{Cu}(298K) = 6.3 \times 10^{-8} \text{ cm}^2/\text{s} ; S_{Cu}(625K) = 3.3 \times 10^{-3} \text{ wt.ppm}$$



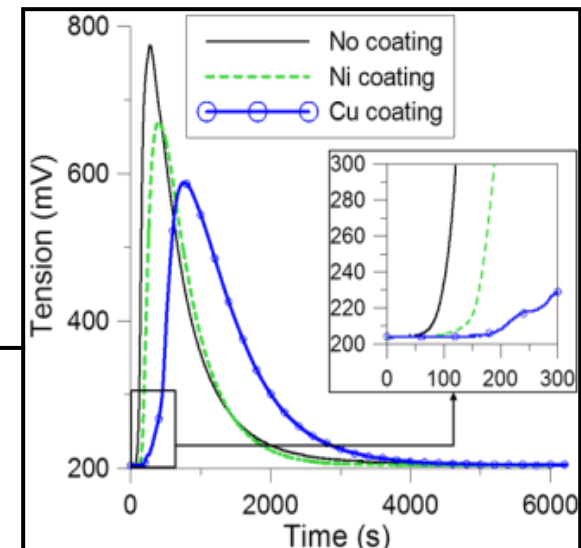
Control of the hydrogen desorption rate by means of Cu or Ni layers electrodeposited prior to gaseous hydrogenation

5. Sample preparation for H charging

- Effects of Cu and Ni layers on total hydrogen concentrations (AISI 430F)

Hydrogenation 723K/200bars/48h

Hydrogen concentration wt.ppm (at.ppm)	Before hydrogenation	After hydrogenation and 2h in N _(L)	After hydrogenation and 144h in N _(L)	After hydrogenation , 144h in N _(L) and 24h at 298K
Ni layer	0.2 (11)	3.5 (194)	3.2 (178)	3.3 (183)
No coating	<0.1 (0)	3.9 (216)	3.8 (210)	3.8 (210)
Cu layer	<0.1 (0)	4.3 (238)	4.3 (238)	4.3 (238)

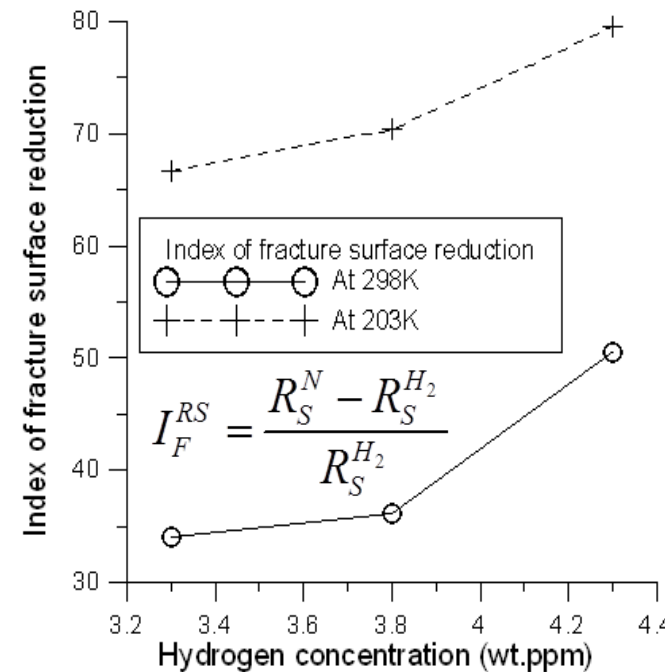
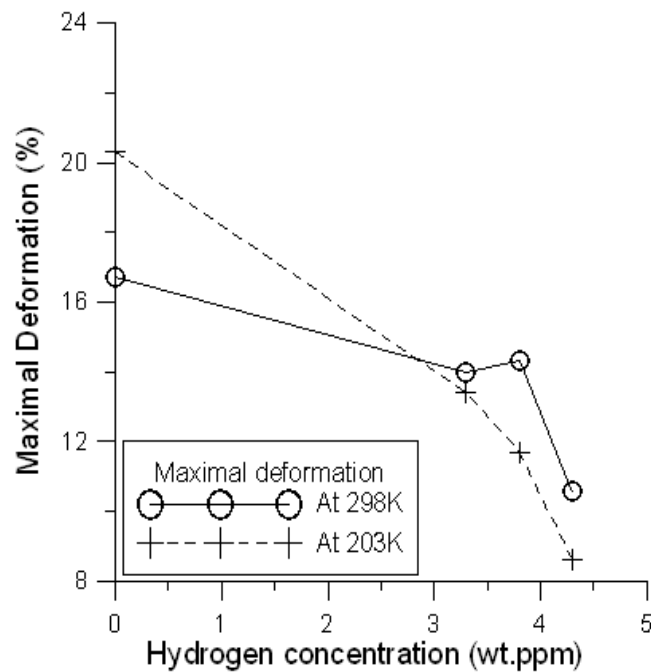


- > Desorption kinetics controlled by hydrogen solubility in the electrodeposited metal
- > The coatings allow adjusting precisely the hydrogen concentrations in a reproducible way for given hydrogenation conditions (pressure, temperature, time)
- > Hydrogen neither desorbs in liquid nitrogen, nor after exposure at room temperature => Subsequent mechanical testing is feasible

5. Sample preparation for H charging

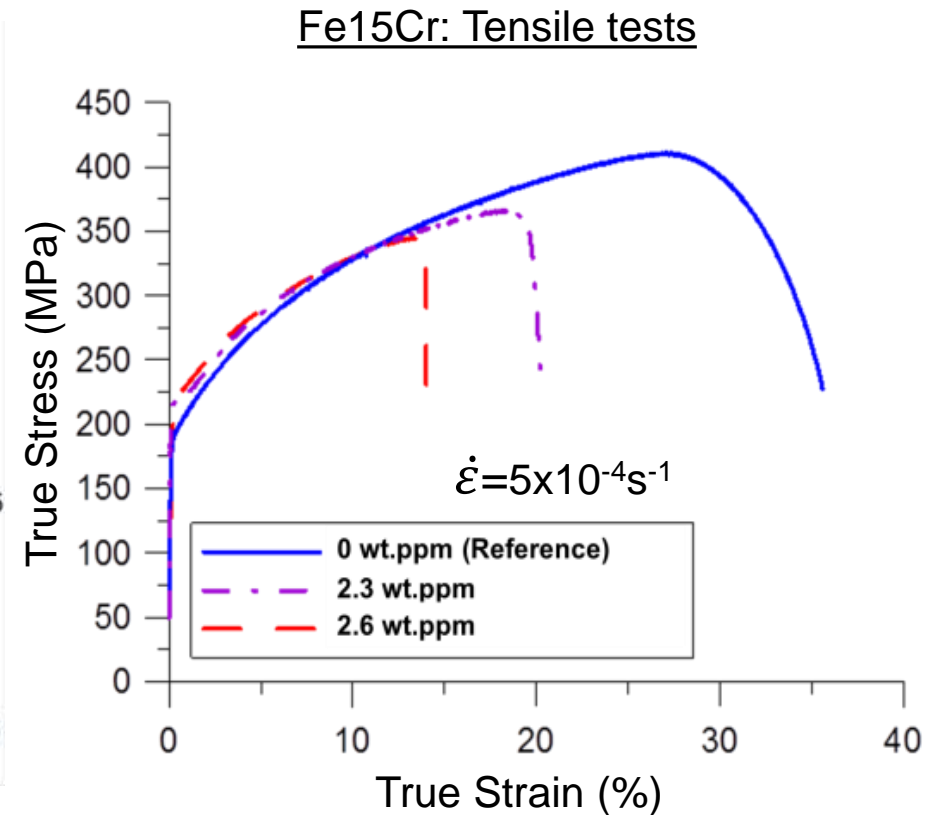
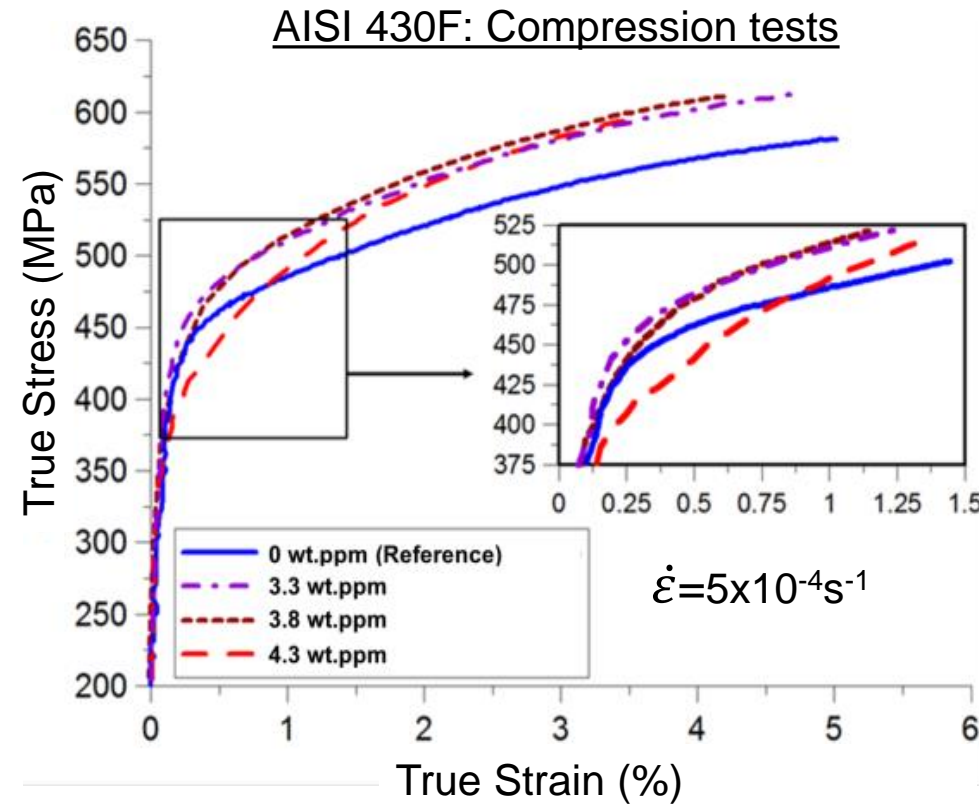
- Consequences on hydrogen embrittlement (AISI 430F)

Tensile strength specimen coated and hydrogenated at 723K/200bars/48h and tested at 298K and 203K



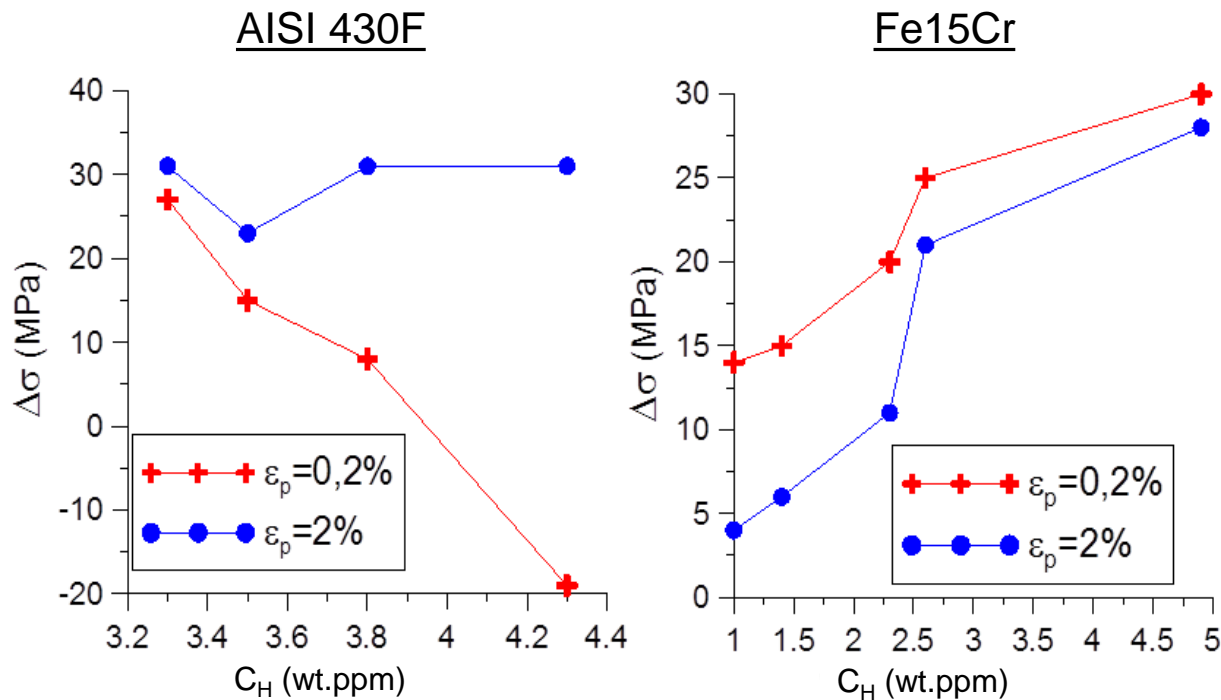
Macroscopic embrittlement is an increasing function of H concentration

5. H-effects on the uniaxial response at 298K

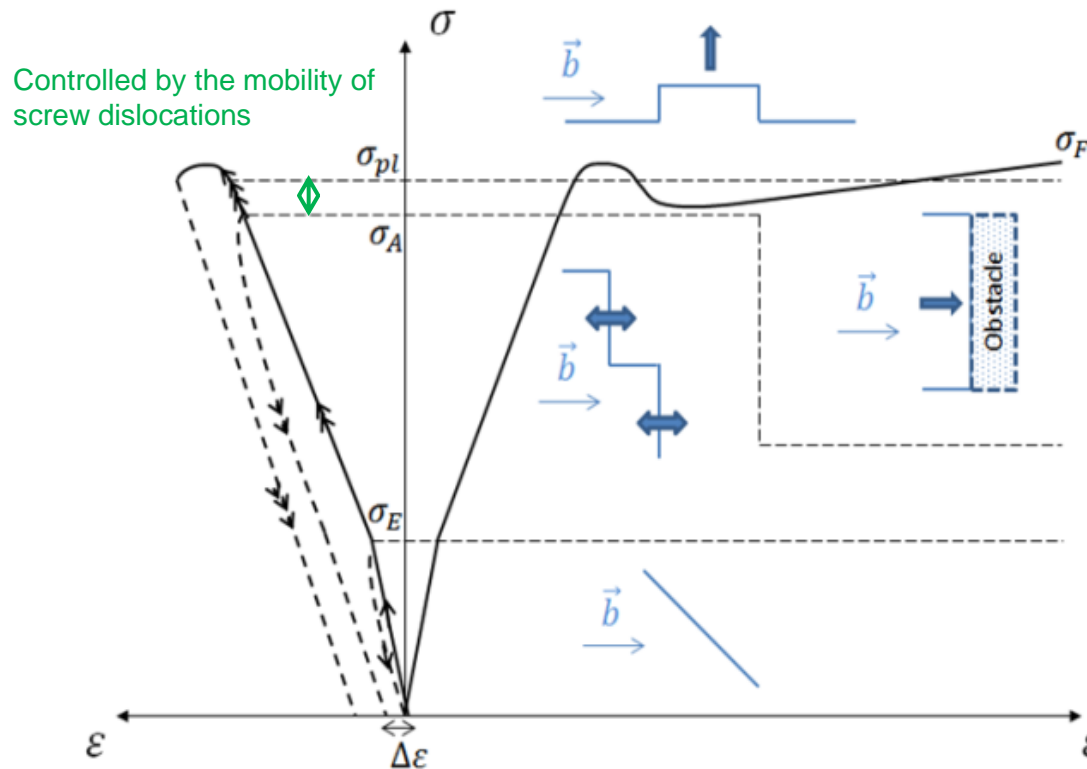


The order of magnitude of the hydrogen effects on the flow stress is 10MPa/wt.ppm

5. H-effects on the uniaxial response at 298K



5. Microyielding and dislocation multiplication in pure iron

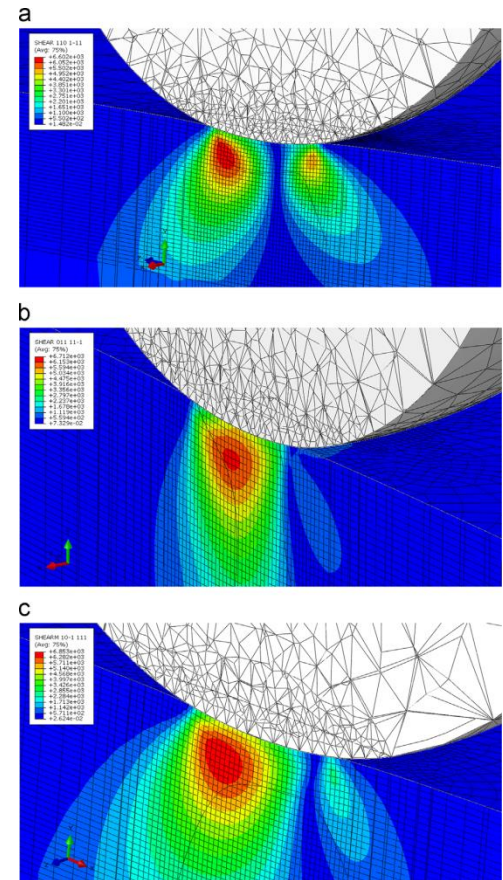
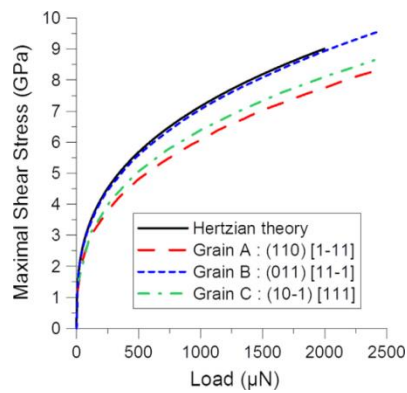
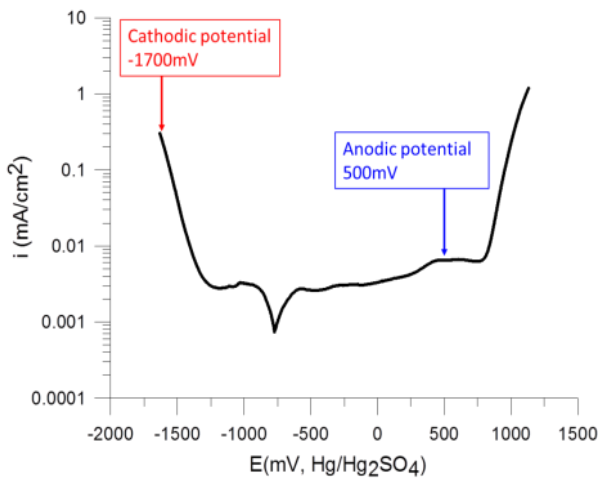
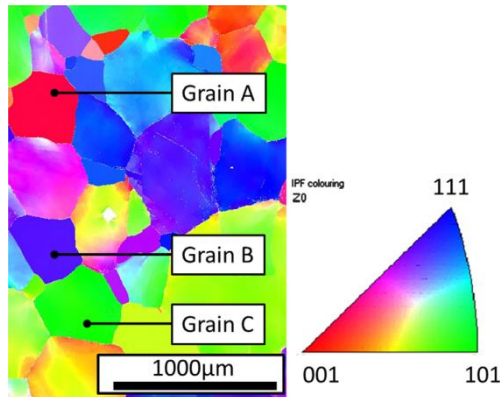
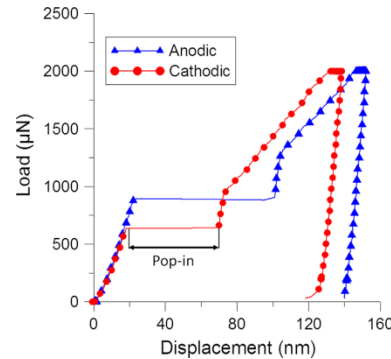


σ_E : Elastic limit
 σ_A : Anelastic limit
 σ_{pl} : Proportional limit

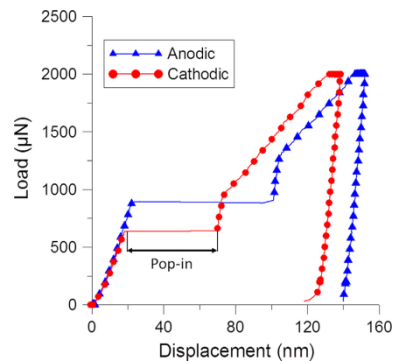
[Solomon, 1971]

[Brown, 1962]

5. Dislocation nucleation in Fe-15Cr

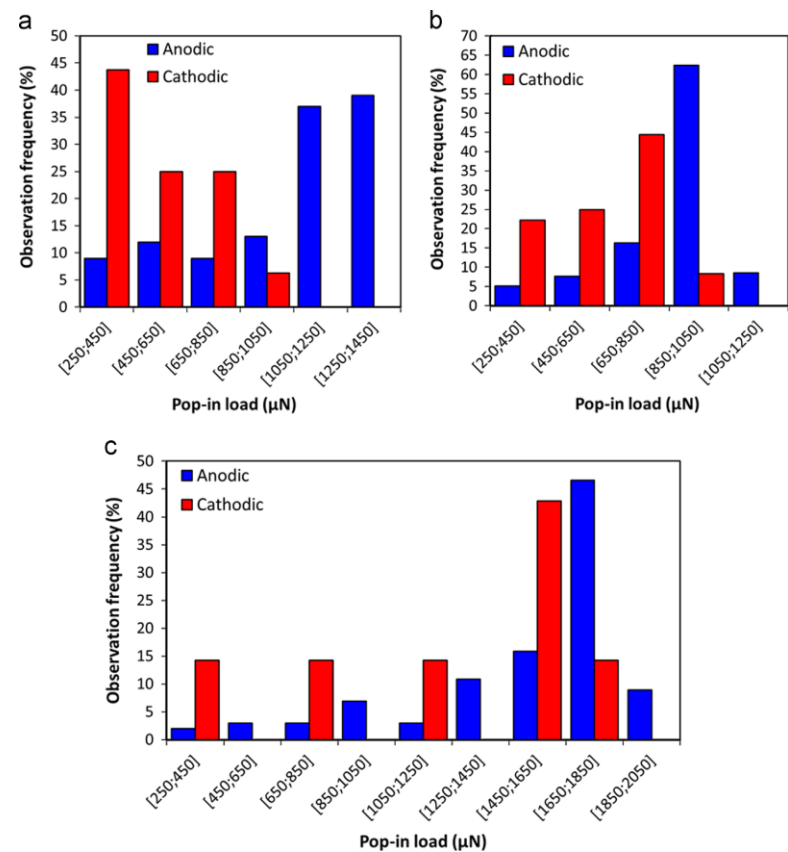


5. Dislocation nucleation in Fe-15Cr



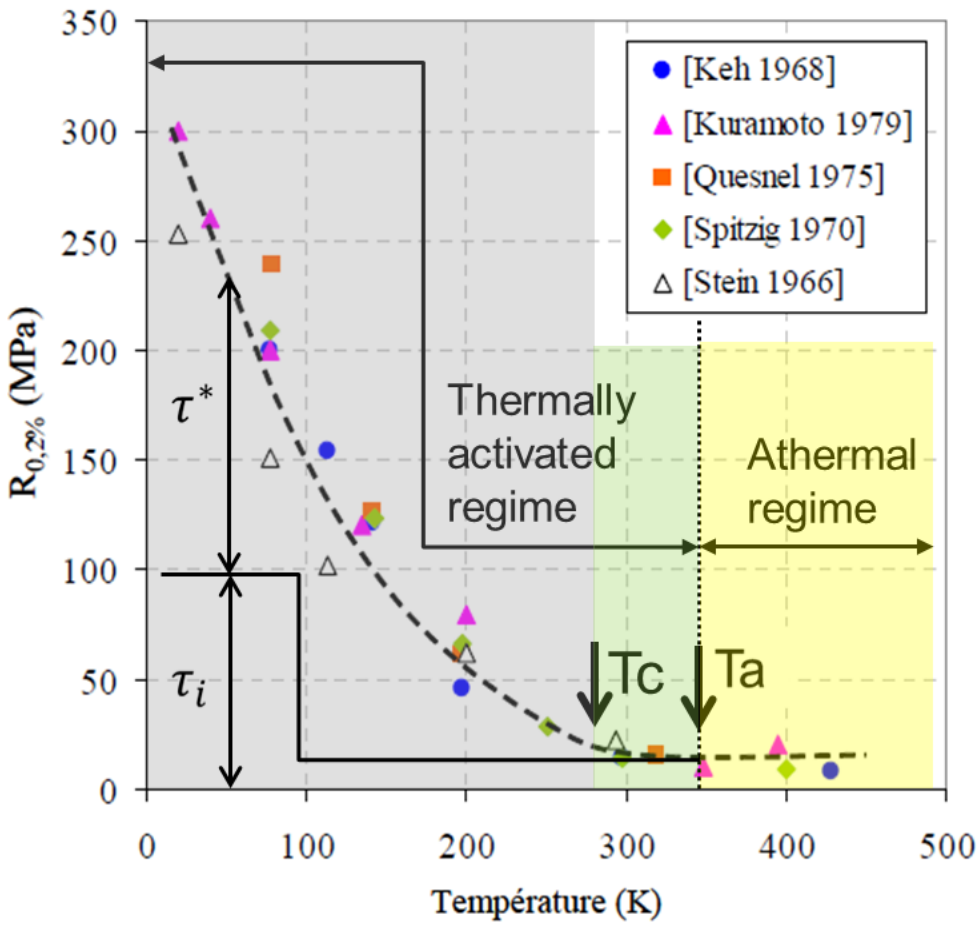
Resolved shear stresses corresponding to the pop-in loads in grains A, B and C under different polarizations.

		Slip system	τ_{pop-in} (GPa)	τ_{pop-in}/μ
Grain A	Anodic	(110)[1-11]	6.21	1/13
	Cathodic		4.98	1/17
Grain B	Anodic	(011)[11-1]	6.75	1/12
	Cathodic		5.98	1/14
Grain C	Anodic	(10-1)[111]	7.10	1/12
	Cathodic		6.50	1/13



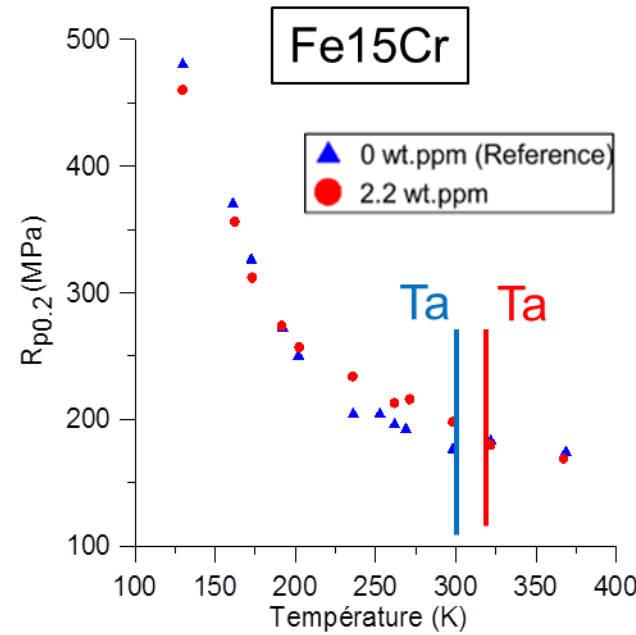
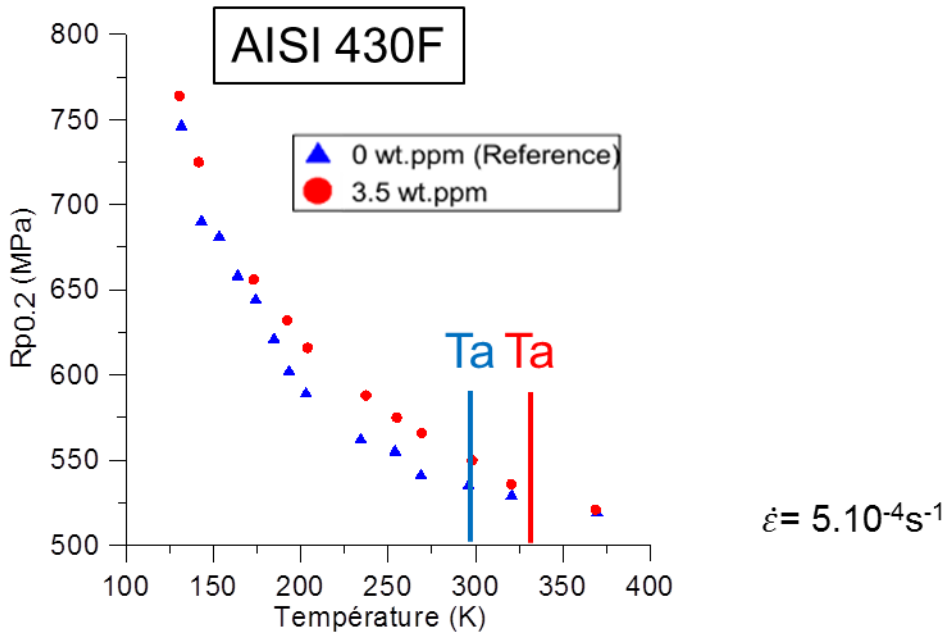
- > CRSS values ($\sim \mu/12-15$) confirm that we are dealing with homogeneous dislocation nucleation
- > They are decreased by 10 to 20% under cathodic polarization

5. Thermally activated regime in α -Fe single crystals



- $T < T_c$: Screw segments are straight and move by double kink nucleation and propagation (1 double kink per dislocation line) due to the very high lattice friction
- $T_c < T < T_a$: Nucleation of several double kinks per dislocation line. Thanks to the thermal activation, the screw segments bow slightly out and the interactions with the forest dislocations are no longer negligible.
- $T > T_a$: The lattice friction is completely rubbed out by the thermal activation, screw and edge segments have similar mobilities and undergo the line tension model, like in F.C.C materials

5. H-effects on the mobility of screw dislocations



AISI 430F	Ta	σ_i (373K)
0wt.ppm	300K	519 MPa
3,5wt.ppm	330K	521MPa

Fe15Cr	Ta	σ_i (373K)
0wt.ppm	300K	174 MPa
2,2wt.ppm	320K	169MPa

Hydrogen in solid solution shifts Ta towards higher temperatures with the order of magnitude of 10K/wt.ppm in the ferritic alloys and decreases the internal stress ($\approx -5 \text{ MPa}$) for hydrogen concentrations of 2-3wt.ppm

5. H-effects on the mobility of screw dislocations

AISI 430F

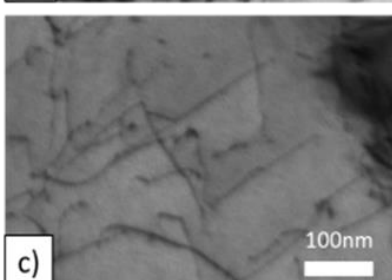
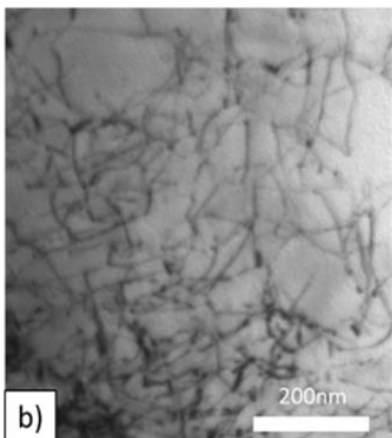
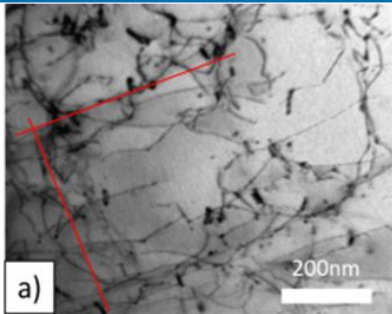
Reference (0wt.ppm)

$\varepsilon_p = 2\% \text{ at } 133K$

Preferential orientations

Entangled dislocations,
curvatures appear

Straight segments

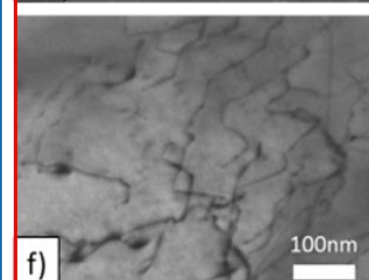
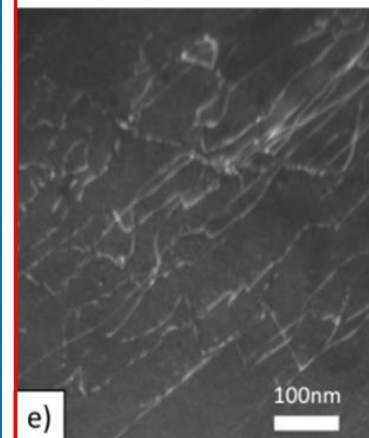
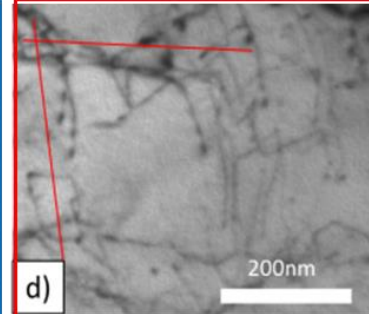


AISI 430F

Hydrogenated
(3,5wt.ppm)
 $\varepsilon_p = 2\% \text{ à } 133K$

Preferencial orientations

Straight dislocations,
parallel structures



High density of double-kinks, typical of thermally activated regime

5. Thermal activation in the low temperature regime of b.c.c. crystals

$$\tau(T, \dot{\varepsilon}) = \tau^*(T, \dot{\varepsilon}) + \tau_i$$

τ^* : Effective stress necessary to overcome obstacles in a thermally activated way (short range interactions: precipitates, lattice friction...)

τ_i : Internal stress necessary to overcome long range interactions (elastic interactions: forest dislocations...)

Mobility of screw segments and strain rate:

$$v_{screw} = b \frac{L}{l_c} v_D \frac{b}{l_c} \exp\left(\frac{-\Delta H(\tau^*)}{k_B T}\right)$$

$$\dot{\gamma} = \rho_m b v_{screw} \quad (\text{Orowan})$$

$$\dot{\gamma} = \dot{\gamma}_0 \exp\left(\frac{-\Delta H(\tau^*)}{k_B T}\right)$$

$\Delta H(\tau^*)$: Double kink nucleation enthalpy

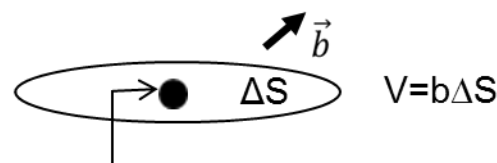
v_{screw} : Mobility of screw segments

Determination of the double kink nucleation enthalpy:

$$\Delta H(\tau^*) = - \int_{\tau_0^*}^{\tau^*} V(\tau^*) d\tau^*$$

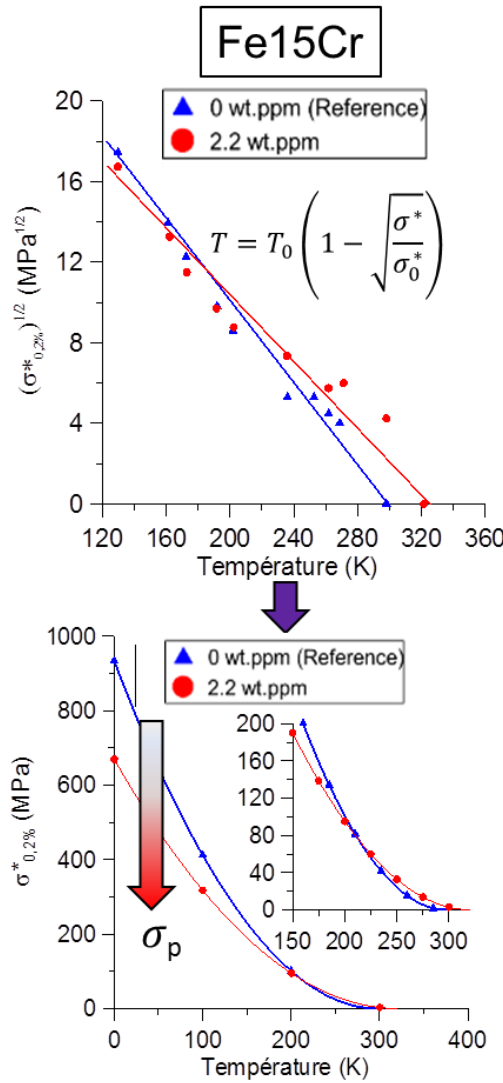
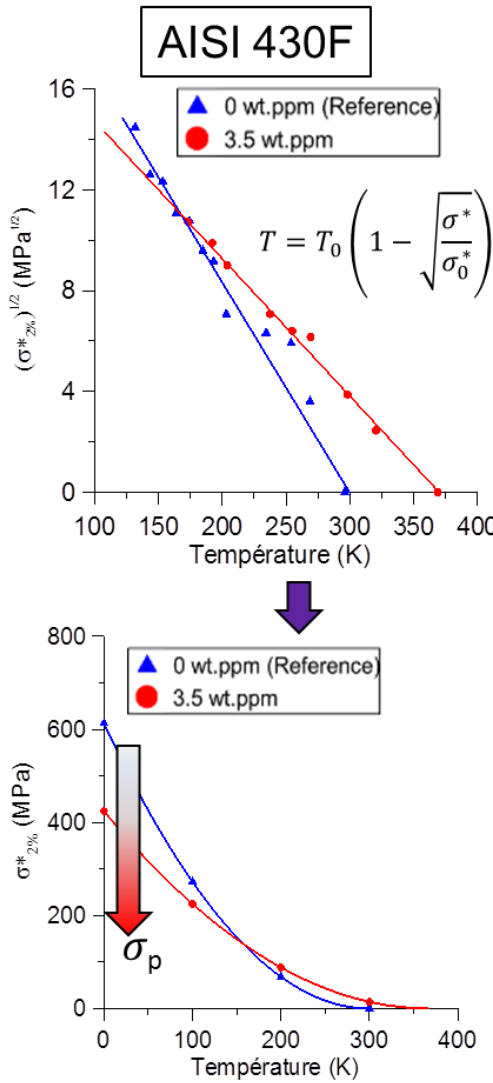
V : Activation volume

τ_0^* : Effective stress at 0K
(Peierls stress)



Obstacle to be overcome by thermal activation

5. Experimental identification of thermal activation parameters



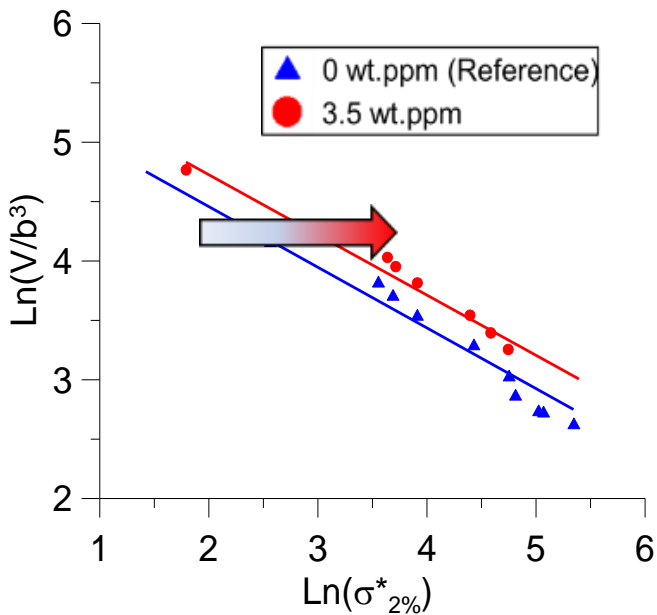
The effective stress corresponds to a plastic deformation of 2% in AISI 430F and of 0.2% in Fe15Cr.

[Smidt, 1969]
[Braillon, 1978]

Hydrogen decreases the effective stress at 0K (extrapolated) by 200MPa in both of the alloys.

5. Experimental identification of thermal activation parameters

AISI 430F



$$V = b^3 \left(\frac{\sigma_c^*}{\sigma_{2\%}^*} \right)^{1/2}$$

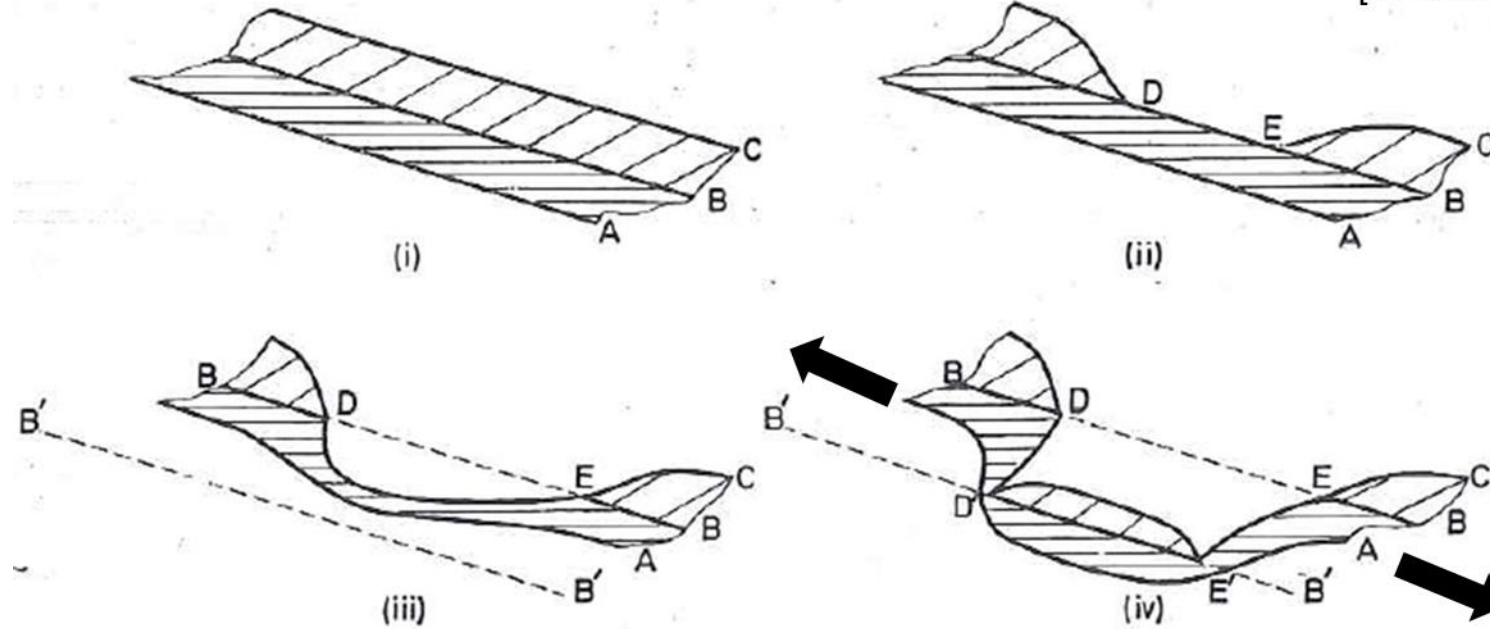
[Smidt, 1969]
[Braillon, 1978]

$$\Delta H(\sigma^*) = - \int_{\sigma_0^*}^{\sigma^*} V(\sigma^*) d\sigma^*$$

In both alloys, the evolution of the effective stress with the temperature, and the evolution of the activation volume with the effective stress are consistent with known results in pure iron [Smidt, 1969].

5. Double kink nucleation and propagation at the microscopic scale

[Duesbery, 1968]



$$\Delta H = 2E_{1d} + E_{int} - W \quad [\text{Hirth, 1982}]$$

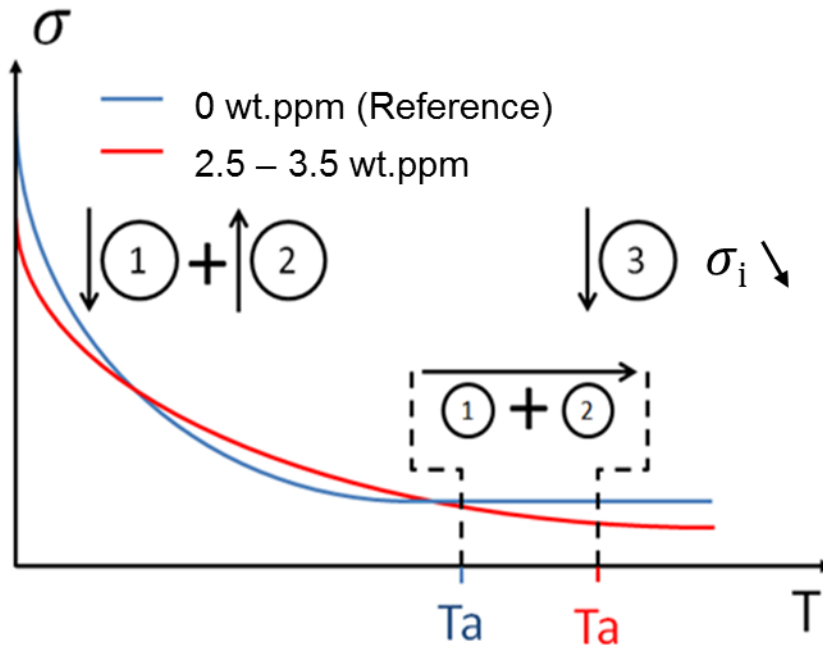
ΔH : Double kink nucleation enthalpy

E_{1d} : Energy of a kink

E_{int} : Interaction energy of the dislocations segments

W : Work induced by the applied stress

5. Interpretation in terms of H-effects on partial recombination and on double kink nucleation



$$\left\{ \begin{array}{l} \dot{\varepsilon} = \dot{\varepsilon}_0 \exp \left(\frac{-\Delta G(\sigma^*)}{kT} \right) \\ \dot{\varepsilon}_0 = \frac{\rho_m b^3 v_D L}{l_c^2} \end{array} \right.$$

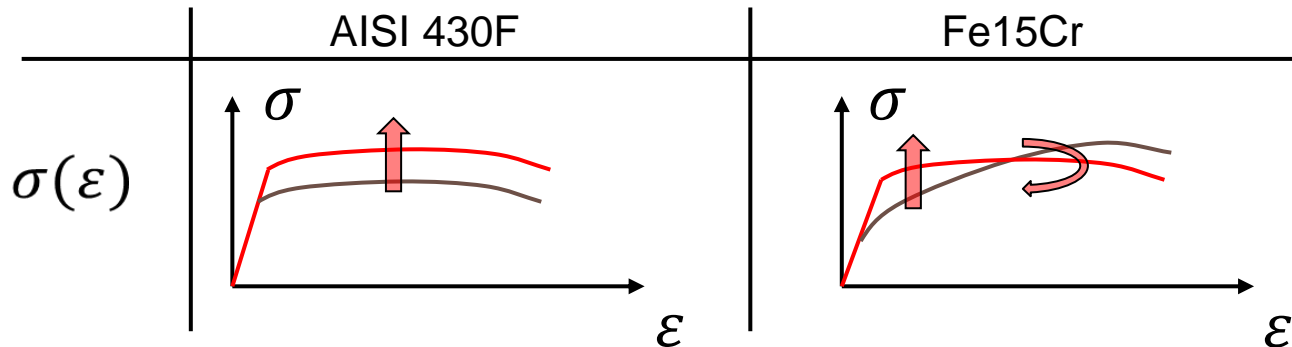
1 2 → $l_c \uparrow$

- ① Hydrogen promotes double kink nucleation: Softening effect
- ② Hydrogen hinders partial recombination (sessile to glissile): Hardening effect
- ③ Shielding effect (elastic interactions): Softening effect

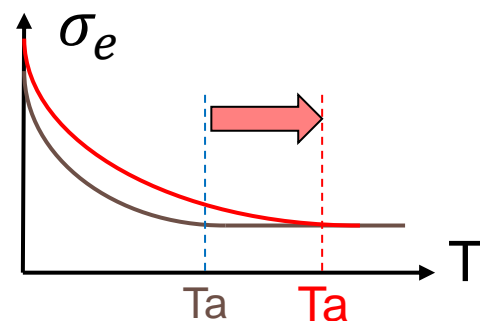
5. Summary

1. Electrodeposited layers of copper and nickel are provide some control over the H content in tensile specimens of H-charged b.c.c. iron

2. Hydrogen effects on tensile properties



3. Hydrogen effect on the athermal temperature T_a (AISI 430F)



Conclusions

1. Solute drag of H atmospheres :

- > Hardening contribution to the flow stress, at room temperature for ordinary strain rates (15-20 MPa for $C_H = 1500-2000$ at. ppm in pure Ni and binary Ni-16Cr)

2. Modelling H-effects at the discrete dislocation scale:

- > Use of the dimensionless “screening index”
- > H-effects on line energy and line tension account for several important reaction mechanisms (multiplication, junction formation and stability ...)
- > The X-slip probability is a mixture of elastic and atomistic properties (SFE and Saddle point configuration energy) and cannot be modelled entirely at this scale

3. Tensile tests on single crystals :

- > Among all the elementary plasticity mechanisms that are liable to H-effects, cross-slip is the one that has the most practical consequences on the tensile response in fcc alloys

Conclusions (cont...)

4. Flow localization in austenitic stainless steels:
 - > Even alloys with a low SFE experience an increase of slip planarity & localization
 - > Statistical measurements and detailed crystal plasticity modelling allow for the quantification of this effect
5. Experiments are increasingly difficult to carry out in bcc iron, but the control of the H-content via electrodeposited copper yields valuable quantitative results
6. H-effects on the flow stress of the order of 20 MPa are obtained with 2-3 ppm of solute H in bcc iron, versus ~ 2000 ppm in fcc nickel or austenitic stainless steels
➔ although the basic ingredients are the same, this cannot be rationalized with one single (simple) mechanism – weighting the # contributions requires a closer look at detailed plasticity mechanisms

Consequences on fracture (work in progress)

- > “Reduced ductility” in, e.g.: austenitic stainless steels
 - > Effects on slip localization provide a straightforward explanation: shear instability of the ligaments between microvoids. Quantitative models are available for this mechanism
(e.g. : Liang, Y., Ahn, D. C., Sofronis, P., *Mechanics of Materials*, 40(2008) p.115)
- > Brittle Intergranular fracture
 - > Slip localization may participate in the fracture process by increasing the “wedge effect” of slip bands emerging at a grain boundary, but this effect alone is not sufficient to cause IG fracture in ductile materials. Some decrease of GB cohesion is required.
→ need to model the effects of dynamic hydrogen trapping at grain boundaries (MD, using EAM and empirical potentials).

Consequences on fracture (work in progress)

- > **Brittle Transgranular fracture**
 - > **fcc alloys:** Effects on the multiplication, line tension and junction strength will affect both the dynamics of crack-tip shielding and crack blunting, but the net effects are not intuitive because contributions of both signs may appear and need to be quantified
 - > **The available results may be readily incorporated in Discrete Dislocation Dynamics (DDD) simulations of crack-tip plasticity to quantify H-effects on fracture at the grain scale**
(Tanguy, Razafindrazaka, Delafosse, Acta Mat.56(2008)p.2441)
 - > **In bcc alloys :** the thermally activated mobility of screw dislocations is known to be central in the DBT. First quantitative data on H-effects have been obtained (e.g.: **shift of the athermal T° towards higher values**). Compared to fcc : importance of core effects (as opposed to remote elastic interactions). Need to be investigated further

Acknowledgements

- Xavier Faugeas (LEMMA, Univ. La Rochelle, France)
- Dôme Tanguy (EMSE & Univ Lyon I, France)
- Isabelle Aubert (LMP, Univ. Bordeaux, France)
- Jean-Marc Olive (LMP, Univ. Bordeaux, France & Hydrogenius Center, Univ. Kyushu, Japan)
- Petros Sofronis (Univ. of Illinois)
- Jacques Chêne (Commissariat à l'Energie Atomique, Saclay, France)
- Afroz Barnoush (NTNU, Norway)

Former PhD students @ EMSE :

- Jean-Philippe Chateau
- Gouenou Girardin
- Mialy Razafindrazaka
- Vincent Gaspard
- Flavien Vucko